



**HAL**  
open science

## The sirtuin SIRT6 regulates stress granule formation in *C. elegans* and mammals

M. Jedrusik-Bode, M. Studencka, C. Smolka, T. Baumann, H. Schmidt, J. Kampf, F. Paap, S. Martin, J. Tazi, K. M. Muller, et al.

► **To cite this version:**

M. Jedrusik-Bode, M. Studencka, C. Smolka, T. Baumann, H. Schmidt, et al.. The sirtuin SIRT6 regulates stress granule formation in *C. elegans* and mammals. *Journal of Cell Science*, 2013, 126 (Pt 22), pp.5166–77. 10.1242/jcs.130708 . hal-02191618

**HAL Id: hal-02191618**

**<https://hal.science/hal-02191618>**

Submitted on 1 Jun 2021

**HAL** is a multi-disciplinary open access archive for the deposit and dissemination of scientific research documents, whether they are published or not. The documents may come from teaching and research institutions in France or abroad, or from public or private research centers.

L'archive ouverte pluridisciplinaire **HAL**, est destinée au dépôt et à la diffusion de documents scientifiques de niveau recherche, publiés ou non, émanant des établissements d'enseignement et de recherche français ou étrangers, des laboratoires publics ou privés.



Distributed under a Creative Commons Attribution 4.0 International License

# The sirtuin SIRT6 regulates stress granule formation in *C. elegans* and mammals

Monika Jedrusik-Bode<sup>1,\*</sup>, Maja Studencka<sup>1</sup>, Christian Smolka<sup>2</sup>, Tobias Baumann<sup>3</sup>, Henning Schmidt<sup>4</sup>, Jan Kampf<sup>1</sup>, Franziska Paap<sup>1</sup>, Sophie Martin<sup>5</sup>, Jamal Tazi<sup>5</sup>, Kristian M. Müller<sup>6</sup>, Marcus Krüger<sup>2</sup>, Thomas Braun<sup>2</sup> and Eva Bober<sup>2,\*</sup>

<sup>1</sup>Max Planck Institute for Biophysical Chemistry, Epigenetics in *C. elegans* group, Am Faßberg 11, 37077 Göttingen, Germany

<sup>2</sup>Max Planck Institute for Heart and Lung Research, Department of Cardiac Development and Remodeling, Ludwigstr. 43, 61231 Bad Nauheim, Germany

<sup>3</sup>Institute of Biochemistry and Biology, University of Potsdam, Karl-Liebknecht-Str. 24-25, 14476 Potsdam, Germany

<sup>4</sup>University of Braunschweig, Institute of Genetics, Spielmannstr. 7, 38106 Braunschweig, Germany

<sup>5</sup>Institut de Génétique Moléculaire de Montpellier, Université Montpellier II, 34293 Montpellier, France

<sup>6</sup>Cellular and Molecular Biotechnology, Faculty of Technology, Bielefeld University, 33615 Bielefeld, Germany

\*Authors for correspondence (mjedrus@gwdg.de; eva.bober@mpi-bn.mpg.de)

Accepted 19 August 2013

Journal of Cell Science 126, 5166–5177

© 2013. Published by The Company of Biologists Ltd

doi: 10.1242/jcs.130708

## Summary

SIRT6 is a NAD<sup>+</sup>-dependent deacetylase that modulates chromatin structure and safeguards genomic stability. Until now, SIRT6 has been assigned to the nucleus and only nuclear targets of SIRT6 are known. Here, we demonstrate that in response to stress, *C. elegans* SIR-2.4 and its mammalian orthologue SIRT6 localize to cytoplasmic stress granules, interact with various stress granule components and induce their assembly. Loss of SIRT6 or inhibition of its catalytic activity in mouse embryonic fibroblasts impairs stress granule formation and delays disassembly during recovery, whereas deficiency of SIR-2.4 diminishes maintenance of P granules and decreases survival of *C. elegans* under stress conditions. Our findings uncover a novel, evolutionary conserved function of SIRT6 in the maintenance of stress granules in response to stress.

**Key words:** *C. elegans*, G3BP, SIRT6, Sirtuins, Stress, Stress granules

## Introduction

All organisms sense and respond to environmental and physiological stress by inducing dynamic changes within the nucleus and cytoplasm. Stress responses are complex processes, which are essential for cellular survival. The physiological relevance is reflected in elaborate control mechanisms, which manage stress responses at different levels, including transcription, translation and stability of RNAs and proteins (Kourtis and Tavernarakis, 2011). Cellular stress in eukaryotic cells in response to heat shock, nutrient deprivation or oxidative damage often leads to the formation of cytoplasmic RNA–protein complexes, which are referred to as stress granules (Anderson and Kedersha, 2009). Stress granules contain non-translating mRNAs and many proteins involved in translation (Anderson and Kedersha, 2006). They have been linked to apoptosis, aging and development of degenerative diseases; however, their exact biological function is still a subject of controversy (Buchan and Parker, 2009).

Silent information regulator 2 (SIR-2) proteins, also termed sirtuins, are highly conserved NAD<sup>+</sup>-dependent protein deacetylases that regulate various cellular activities, in particular during cellular stress and disease processes. Decisive functions of sirtuins have been described in different cellular pathways regulating transcriptional repression, aging, metabolism, cell

defences against DNA damage and apoptosis (Haigis and Guarente, 2006). Sirtuins are active in the nucleus as well as in the cytoplasm as part of a salvatory response to stress, resulting in cell survival and extended lifespan in yeast, worms, flies and mice (Tissenbaum and Guarente, 2001; Rogina and Helfand, 2004; Kanfi et al., 2012).

Seven SIR2 homologs (SIRT1–SIRT7) have been identified in mammals. They share the conserved sirtuin domain but vary in subcellular localization and function. SIRT1, SIRT6 and SIRT7 localize to the nucleus; SIRT3, SIRT4 and SIRT5 are mitochondrial, whereas SIRT2 is predominantly cytoplasmic (Haigis and Guarente, 2006). The mammalian SIRT6 recapitulates many of the biological functions of SIR-2 and its homologues in fly and worm. At the molecular level, SIRT6 regulates the expression of a large number of stress-responsive and metabolism-related genes, promotes genomic stability (Kawahara et al., 2009; Mostoslavsky et al., 2006) and stimulates base excision (Mostoslavsky et al., 2006) as well as repair of double-strand breaks in DNA (McCord et al., 2009; Kaidi et al., 2010). To date, most of the molecular functions of SIRT6 have been ascribed to its deacetylase activity and are linked to SIRT6 chromatin-modifying activities; SIRT6 is known to deacetylate H3K9 (Michishita et al., 2008), H3K56 (Michishita et al., 2009) and CtIP *in vivo* (Kaidi et al., 2010). Recently, it has also been reported that SIRT6 mono-ADP ribosylates PARP1 to stimulate DNA repair in response to oxidative stress (Mao et al., 2011). A role of sirtuins in stress granule assembly and survival has not been examined so far.

The genome of *C. elegans* encodes four different SIR-2 variants (*sir-2.1*, *sir-2.2/2.3* and *sir-2.4*) with high sequence similarities to mammalian sirtuins (SIRT1, SIRT4 and SIRT6). SIR-2.1 is the best characterized protein of the four *C. elegans* SIR-2 variants and is involved in germline silencing of multicopy transgenic arrays, modulation of transcription of genes in response to stress, as well as extension of life span (Jedrusik and Schulze, 2003; Tissenbaum and Guarente, 2001). SIR-2.4, a SIRT6 orthologue, was recently identified as a new factor in stress resistance and regulator of DAF-16 (FoxO transcription factor) acetylation by inhibition of the acetyltransferase CBP1 (Chiang et al., 2012).

Here, we investigated the role of *C. elegans* SIR-2.4 and its mammalian orthologue SIRT6 in the formation and function of stress granules. We found that SIRT6 translocates into the cytoplasm under stress and regulates formation as well as disassembly of stress granules. Importantly, we showed that the deacetylase activity of SIRT6 promotes dephosphorylation of G3BP at serine 149 (Ser149), thereby influencing assembly of stress granules and cell viability. The SIRT6 orthologue in *C. elegans*, SIR-2.4, is necessary for efficient formation of P granules and extended survival under heat stress. Our results uncover a novel, evolutionary conserved function of SIRT6 in mechanisms of stress protection.

## Results

### SIR-2.4 regulates the stress response

Previous results from our laboratory and others suggested that knockdown or knockout of *sir-2.4* renders *C. elegans* hypersensitive to heat shock (Chiang et al., 2012). Incubation of animals at a non-permissive temperature (36.5°C) confirmed that *sir-2.4*-depleted 3-day-old hermaphrodites lived for a shorter time (32%;  $P < 0.0001$ ) than wild-type hermaphrodites (Fig. 1). To examine whether *sir-2.4* regulates stress response and longevity in a cell-autonomous manner, we inactivated *sir-2.4* specifically in the germline of *C. elegans* using the *rff-1(pk1417)* strain, which permits RNAi activity in the germline but not in somatic cells (Sijen et al., 2001). We found that knockdown of *sir-2.4* in *rff-1(pk1417)* mutant animals (22%,  $P < 0.0001$ )

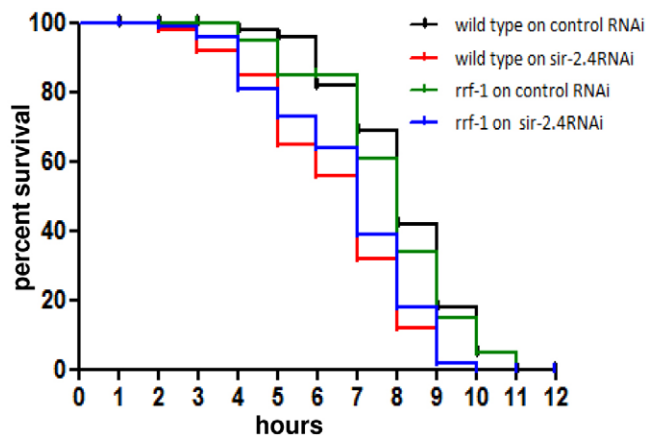


**Fig. 1. Loss of SIR-2.4 causes increased stress sensitivity.**

Thermotolerance assay of 3-day-old hermaphrodites (mean values of three independent experiments, 120 worms used in each analysis). Constitutional and germline-specific knockdown of SIR-2.4 decrease survival under heat stress.

decreased lifespan after heat stress compared with control animals, implying an important role of SIR-2.4 in the regulation of the stress response in the germline (Fig. 1).

### SIR-2.4 interacts with K08F4.2, an orthologue of the mammalian G3BP

To gain mechanistic insights into the function of SIR-2.4 we performed a yeast two-hybrid screen (Y2HS) using SIR-2.4 as bait. Unexpectedly, we found that SIR-2.4 interacted with K08F4.2, which represents the *C. elegans* orthologue of the mammalian Ras-GTPase-activating protein G3BP (79% amino acid homology). G3BP is a component of mammalian stress granules that form in response to heat shock or oxidative stress (Tourrière et al., 2003; Anderson and Kedersha, 2006). In addition, G3BP plays an important role in the regulation of cell proliferation and survival, and links signal transduction to RNA metabolism (Irvine et al., 2004).

To verify the interaction between SIR-2.4 and K08F4.2, we expressed tagged proteins in NIH3T3 mouse embryonic fibroblasts (MEFs) and performed colocalization and coimmunoprecipitation experiments. We observed that SIR-2.4::GFP and K08F4.2::mCherry were diffusely distributed in NIH3T3 cells before stress, but were recruited to the same bright cytoplasmic foci in response to heat shock (Fig. 2A). We found that K08F4.2 and SIR-2.4 fusion proteins efficiently co-precipitated in extracts prepared from unstressed and stressed cells (Fig. 2B). Another known *C. elegans* SIR-2 variant, the SIR-2.2 fusion protein did not associate with K08F4.2::mCherry under the same experimental conditions (Fig. 2B).

To investigate whether SIR-2.4::GFP foci represent stress granules (Fig. 2A), we stained NIH3T3 cells for G3BP, the mammalian counterpart of K08F4.2. G3BP decorated SIR-2.4-positive cytoplasmic aggregates, suggesting that SIR-2.4 is recruited into mammalian stress granules upon heat shock (Fig. 2C). In similar conditions, GFP alone did not localize into G3BP foci (supplementary material Fig. S1).

### SIR-2.4 is localized to P granules, which are related to mammalian stress granules

Because P granules in *C. elegans* encompass properties of mammalian stress granules (Anderson and Kedersha, 2006) and SIR-2.4 colocalizes with the stress granule marker G3BP in heat-shock-treated NIH3T3 cells (Fig. 2C), we assumed that SIR-2.4 would also localize to P granules in *C. elegans*. In fact, we detected SIR-2.4 in small cytoplasmic granules of germline cells colocalizing with PGL-1, PGL-3 and GLH-1.2, which are all constitutive components of the germline-specific P granules independent of temperature (Fig. 2D). In addition, we identified endogenous and GFP-tagged SIR-2.4 in the nucleus, where it predominantly localized to the nuclear envelope (Fig. 2D; supplementary material Fig. S2) and the nuclear pore complex (supplementary material Fig. S2B).

### SIR-2.4 regulates the formation of P granules

Because SIR-2.4 confers resistance to heat shock, and cytoplasmic P granules in oocytes are induced by multiple environmental stresses and by aging (Jud et al., 2008; Pitt et al., 2000), we investigated the relationship between P granule formation in pachytene-stage germ cells and survival of wild-type and *sir-2.4*-depleted mutant animals under heat-shock conditions (36.5°C). Interestingly, depletion of *sir-2.4* caused a

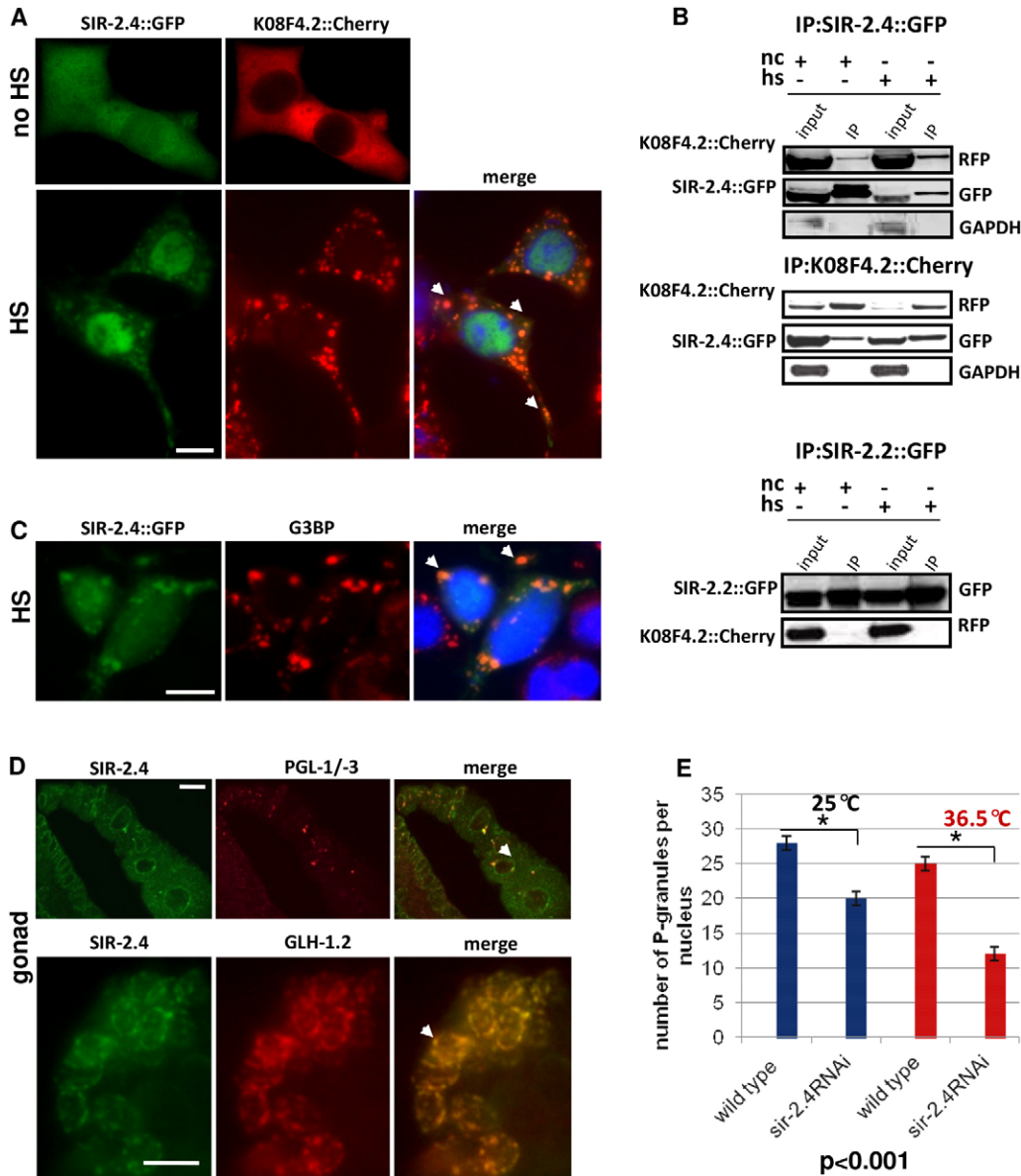


**Fig. 2. *C. elegans* SIR-2.4 interacts with K08F4.2/G3BP and localizes to stress granules.** (A) Distribution pattern of GFP-tagged SIR-2.4 and mCherry-tagged K08F4.2 proteins in unstressed (no HS, no heat shock) and heat shocked (HS) NIH3T3 cells.

Arrowheads indicate the colocalization of SIR-2.4- and K08F4.2-tagged proteins. (B) Co-immunoprecipitation of SIR-2.4 (or SIR-2.2)- and K08F4.2-tagged proteins overexpressed in NIH3T3 cell line at 37°C and 42°C (heat shock); nc, normal condition; hs, heat-shock condition. GAPDH was used as a loading control.

(C) Colocalization of SIR-2.4::GFP with G3BP (arrowheads), a marker for stress granules in stressed NIH3T3 cells. (D) Representative images presenting colocalization of endogenous SIR-2.4 with components of P granules in arrested oocytes using anti-PGL-1/-3 and/or in pachytene-stage germ cells using anti-GLH-1.2 (arrowheads).

(E) Number of P granules found in ten nuclei of pachytene stage germ cells of hermaphrodites growing for 5 hours at 36.5°C. Results are mean values  $\pm$  s.d. of three independent experiments; \* $P$ <0.01 versus wild type at 25°C or 36.5°C. Scale bars: 10  $\mu$ m.

28% reduction of the number of P granules in gonad arms ( $20 \pm 2$ /nucleus) in contrast to wild-type animals at 25°C ( $28 \pm 2$ /nucleus; 32 hermaphrodites were examined in triplicate) (Fig. 2E; supplementary material Fig. S3A; for *sir-2.4*RNAi efficiency, see supplementary material Fig. S3B). Heat-shock treatment resulted in decreased numbers of P granules (52%) in *sir-2.4*-depleted compared with wild-type cells. The reduced viability together with the reduced number of P granules in *sir-2.4*-depleted animals suggests that *sir-2.4* is instrumental to confer resistance to environmental stress probably by regulation of P granule formation, thereby enabling enhanced survival rates.

#### Mammalian SIRT6, an orthologue of SIR-2.4, interacts with stress granule components and relocates to the cytoplasm upon stress

To investigate whether mammalian SIRT6, which shares a 95.5% homology with SIR-2.4, fulfils a similar role as SIR-2.4, we analyzed the function of SIRT6 in stress granule formation.

Immunoprecipitation of SIRT6::YFP stably expressed in SILAC-labeled human embryonic kidney 293 (HEK293) cells followed by quantitative mass spectrometry identified several proteins previously reported to be components of stress granules as an interaction partner of SIRT6. Among the interactors, we found G3BP (an orthologue of *C. elegans* K08F4.2) with 16 unique peptides and 43% sequence coverage, USP-10 (ubiquitin C-terminal hydrolase 10) with 21 peptides and 20% sequence coverage, Caprin-1 (Cytoplasmic activation- and proliferation-associated protein 1) with 12 peptides and 18% sequence coverage as well as PABP-1 (polyadenylate-binding protein 1) with 19 peptides and 10% sequence coverage. Specificity of the interaction between SIRT6::YFP with endogenous stress granule components such as G3BP and PABP1 was validated by coimmunoprecipitation (Fig. 3A). Immunoprecipitation of total cell extracts using GFP antibody recovered G3BP and PABP1 with SIRT6::YFP fusion protein (Fig. 3A). The specificity of the interaction between SIRT6 and G3BP was demonstrated by the

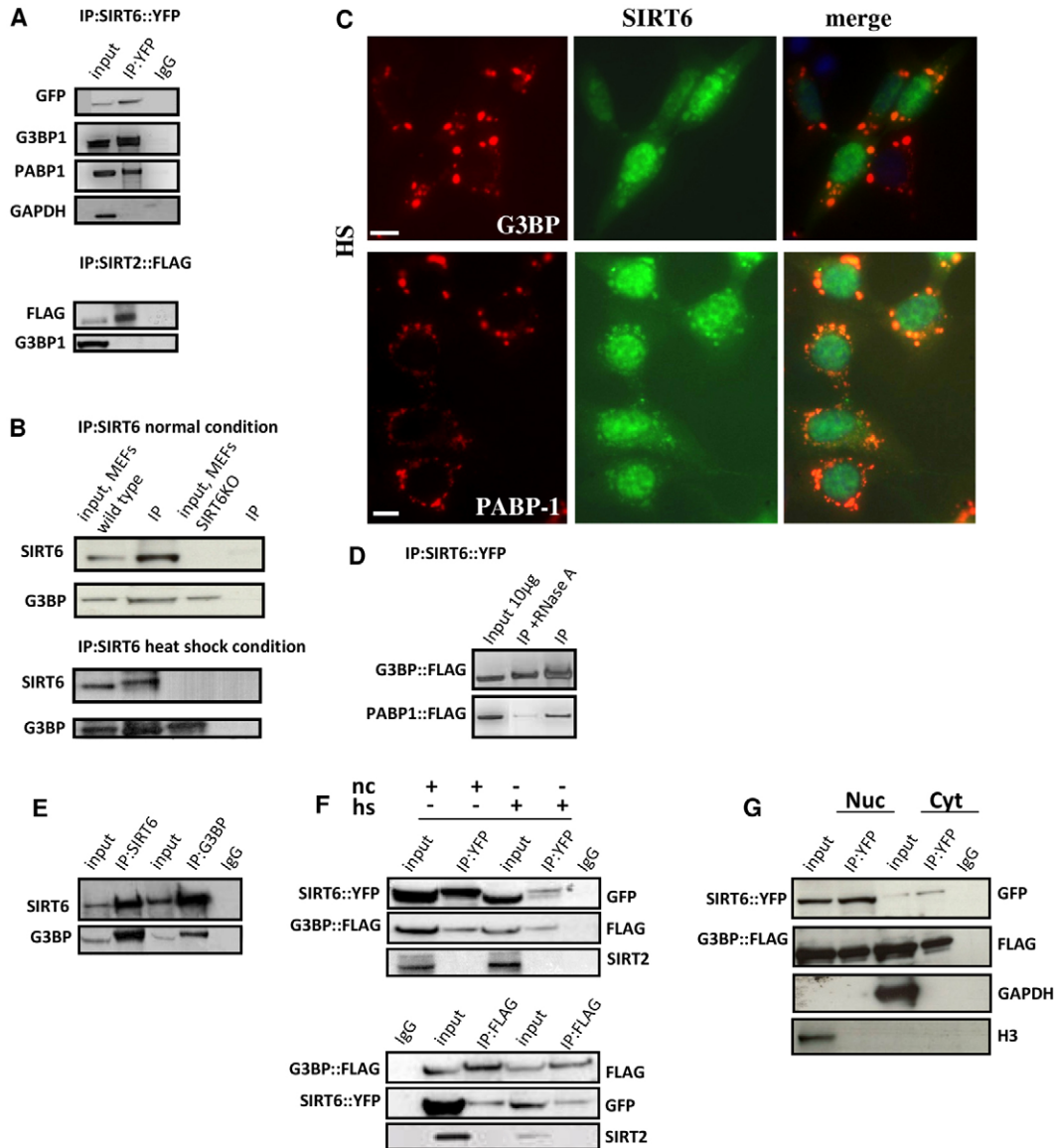


**Fig. 3. SIRT6 co-immunoprecipitates components of mammalian stress granules.** (A) SIRT6::YFP fusion protein co-precipitates endogenous G3BP and PABP-1. SIRT2::FLAG, negative control; GAPDH, loading control. (B) Co-immunoprecipitation of endogenous G3BP using SIRT6 antibody and total cell extracts obtained from wild-type MEFs. SIRT6KO MEFs served as a negative control. (C) Colocalization study of endogenous SIRT6 and markers of stress granules: G3BP or PABP-1 in heat-shocked cells. Scale bars: 10  $\mu$ m. (D) Verification of SIRT6 interaction partners by co-immunoprecipitation before and after RNase A treatment. (E) *In-vitro*-translated G3BP and SIRT6 exhibit reciprocal co-immunoprecipitation as shown in western blots. (F) Western blot analysis showing co-immunoprecipitation of FLAG-tagged G3BP and SIRT6::YFP-fusion proteins expressed in NIH3T3. nc, normal condition; hs, heat-shock condition. SIRT2, control. (G) SIRT6-G3BP association in cytoplasmic and nuclear fraction using heat-shocked NIH3T3 cell lysates which were transfected with G3BP and SIRT6 fusion proteins, fractionated and immunoprecipitated.

lack of binding between G3BP and the other member of the sirtuin family, SIRT2 (Fig. 3A, bottom panel). In addition, we detected endogenous SIRT6 and G3BP in a coimmunoprecipitation assay as evidence of the physiological interaction between SIRT6 and G3BP at 37°C (normal condition) and 42°C (stressed condition) (Fig. 3B). Furthermore, colocalization studies of endogenous SIRT6 and G3BP proteins in unstressed and heat-shock-treated cells revealed that SIRT6 is mainly present in the nucleus of unstressed cells (supplementary material Fig. S4). Exposure to high temperature (42°C) leads to relocalization of SIRT6 and formation of SIRT6-positive cytoplasmic patches throughout the

cytoplasm, which also contain other stress granule markers G3BP or PABP1 (Fig. 3C).

Because G3BP and PABP1 are mRNA binding proteins, we also examined whether RNA is required for binding to SIRT6. Interestingly, coimmunoprecipitation followed by RNase treatment revealed that SIRT6 efficiently bound to PABP1 only in the absence of ribonuclease A, whereas the binding of G3BP to SIRT6 did not depend on RNA (Fig. 3D). The effectiveness of the RNase treatment was also assessed on agarose gel (supplementary material Fig. S5A). Furthermore, we used *in vitro* translated PABP1 as a negative control to demonstrate that

SIRT6 binds to PABP1 in an RNA-dependent manner (supplementary material Fig. S5B). Additionally, co-immunoprecipitation of *in vitro* translated SIRT6 and G3BP indicated that binding of both proteins is most likely direct (Fig. 3E).

To verify whether the relocalization of SIRT6 to stress granules is restricted only to specific forms of environmental stress or is a phenomenon of a specific cell line, we overexpressed SIRT6-tagged protein in NIH3T3 or U2OS cells and used sodium arsenite (AS) treatment or exposure to heat shock. We observed that SIRT6 was recruited into stress granules under all stress stimuli and in both cell lines used in this study (supplementary material Fig. S6). Unexpectedly, the interaction between SIRT6::GFP and G3BP::FLAG appeared to be independent of stress because both proteins efficiently co-precipitated in non-stressed and stressed conditions (Fig. 3F). Biochemical fractionation experiments revealed that SIRT6 and also G3BP are present in the nuclear and cytoplasmic fractions after stress and that they can be found in complex together in both cellular compartments (Fig. 3G).

#### Cytoplasmic localization of SIRT6 is partially dependent on G3BP

To find out whether the interaction between G3BP and SIRT6 regulates recruitment of SIRT6 to stress granules, we overexpressed SIRT6-tagged protein in G3BPKO MEF cells (Fig. 4A). As previously reported, cells lacking G3BP induced significantly fewer large cytoplasmic stress granules as visualized by TIA-1 immunofluorescence (Fig. 4A). Accordingly, we found that these granules also expressed SIRT6 and their number was decreased in G3BPKO MEFs compared with wild-type MEFs. These results suggest that the subcellular redistribution of nuclear SIRT6 to cytoplasmic stress granules undergoes similar regulatory constraints as other proteins typically present in stress granules and that this process is at least partially dependent on G3BP.

We further determined whether new protein synthesis was involved in the heat-shock-induced increase of cytoplasmic SIRT6. Therefore, we preincubated the NIH3T3 cells for 30 minutes with the protein synthesis inhibitor cycloheximide or in control medium (DMSO). Cycloheximide leads to a strong reduction of stress granules, inhibits translational elongation and blocks the disassembly of polysomes (Kedersha et al., 2000). We observed that cycloheximide clearly decreased the fluorescence density of cytoplasmic SIRT6, with respect to those of control conditions. As expected, addition of cycloheximide to stressed cells resulted in partial stress granule disassembly, suggesting that polysome disruption is important for stress granule assembly and incorporation of SIRT6 to these foci (Fig. 4B).

#### SIRT6 undergoes structural rearrangements upon exposure to elevated temperatures

In response to heat shock, many proteins become partially unfolded or misfolded and are retrotranslocated to the cytoplasm, where they are ubiquitinated and degraded by the proteasome (Werner et al., 1996). Because different cell lines were subjected to a continuous 42°C heat shock in most of our experiments, we investigated the influence of temperature on the thermal stability and enzymatic activity of the SIRT6 protein *in vitro*. Fig. 5A shows the thermal denaturation profile of human recombinant SIRT6 as determined by intrinsic tryptophan fluorescence. With the exception of Trp69 (supplementary material Fig. S7), the

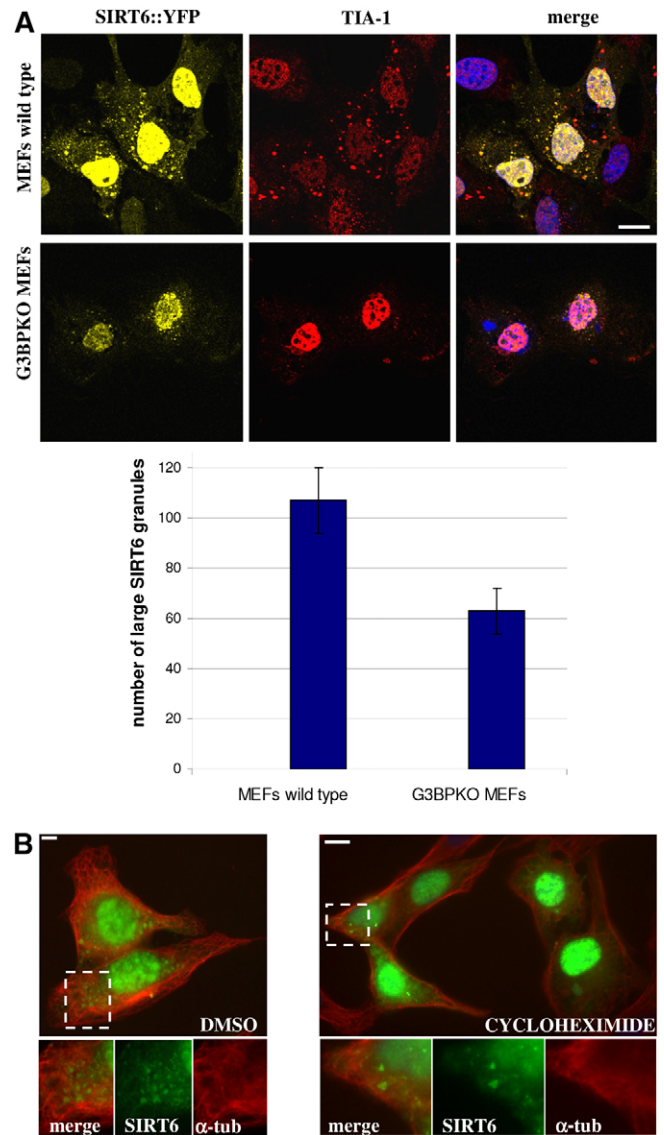


**Fig. 4. G3BP partially regulates SIRT6 recruitment to stress granules.** (A) The presence of large SIRT6::YFP granules in cytoplasm of heat-shocked wild-type MEFs in contrast to G3BP KO MEFs. TIA-1, stress granule marker. Scale bars: 6  $\mu$ m. The graph shows the average size of SIRT6::YFP granules in MEFs. Analysis was based on ten transfected cells. The large class of granules was identified on the basis of size (large, 31–230 pixels<sup>2</sup>). Results are means  $\pm$  s.d. (B) Effect of cycloheximide on cytoplasmic SIRT6 aggregations during heat shock. NIH3T3 cells were exposed to heat shock in the presence of cycloheximide (CHM) or DMSO (control). Representative cells showing partial inhibition of stress granule formation by cycloheximide and the absence of effect by DMSO are depicted.  $\alpha$ -tubulin (tub), control for immunostaining efficiency. Scale bars: 10  $\mu$ m.

other four tryptophan residues of human SIRT6 are located close to the protein surface as evident from protein crystal structures (PDB ID:3K35, 3ZG6; P. W. Pan, A. Dong, J. Min, C. Arrowsmith and A. Edwards, unpublished data; Jiang et al., 2013). Assuming a two-state transition from native to unfolded protein, the thermally induced unfolding reached its midpoint at  $41.8 \pm 0.3^\circ\text{C}$  for protein concentrations of 0.05 and 0.1 mg/ml, respectively. As observed for many proteins, especially those of

more than 150 amino acids in length, the thermal unfolding process was irreversible (Sanchez-Ruiz, 2010; Ganesh et al., 1997). Consequently, no thermodynamic description was performed. In order to follow the unfolding of the protein core, SIRT6 was further subjected to thermal unfolding in the presence of the fluorescent dye Sypro Orange. Differential scanning fluorimetry revealed an onset of thermal unfolding at 41–42°C, with an apparent midpoint at  $45.7 \pm 0.2^\circ\text{C}$  (Fig. 5B). Again, and typical for this dye-binding assay, thermal unfolding was irreversible (Phillips and de la Peña, 2011). Relative to changes in the fluorescence characteristics of tryptophan residues, differential scanning fluorimetry is able to detect the exposure of hydrophobic patches during the unfolding of the protein core (Uniewicz et al., 2010). It is thus conceivable that the midpoint of this process is reached at later stages of thermal unfolding relative to the solvent exposure of the tryptophan residues.

In order to determine the temperature dependence of SIRT6 enzyme activity, the deacetylation of a human p53 substrate peptide by human recombinant SIRT6 was analyzed in the presence of  $\text{NAD}^+$  after heat shock at various temperatures (Fig. 5C). Control samples incubated on ice yielded the same signal of converted substrate as those incubated at  $20^\circ\text{C}$ , which implies that SIRT6 was sufficiently stable for the time period of the assay. Furthermore, a heat shock at  $55^\circ\text{C}$  in the absence of SIRT6 protein did not lead to marked substrate conversion, confirming the stability of the labeled peptide. Although it remained constant at  $25\text{--}38^\circ\text{C}$ , SIRT6 deacetylase activity decreased at a heat-shock temperature above  $38^\circ\text{C}$ . For the irreversible functional inactivation of the enzyme, a half-inactivation temperature of  $43.0 \pm 0.2^\circ\text{C}$  was determined.

As evident from biochemical analysis, human recombinant SIRT6 underwent structural rearrangements upon exposure to elevated temperatures and retained  $\sim 72\%$  enzymatic activity after a heat shock at  $42^\circ\text{C}$ . Apparently, detectable small structural changes took place around  $24^\circ\text{C}$ , which could be interpreted as increased protein compactness, which was indicated by increased tryptophan fluorescence (Fig. 5A) and decreased extrinsic dye fluorescence (Fig. 5B). However, the detailed nature and consequences of these structural changes remain unknown; SIRT6 deacetylase activity does not appear to be affected (compare Fig. 5C).

### Deacetylase activity of SIRT6 is important for G3BP granule formation

Next, we tested whether SIRT6 deficiency affects assembly of G3BP-containing stress granules in stressed cells. In fact, loss of SIRT6 caused changes in the formation of endogenous and overexpressed G3BP foci (Fig. 6A,B). In particular, G3BP::GFP granules had a more diffuse pattern in SIRT6KO MEFs, and showed a size reduction as well as less-defined and more-irregular morphology than wild-type MEFs (Fig. 6B). To analyze whether the ability of SIRT6 to induce formation of G3BP-containing stress granules depended on its enzymatic activity, we used nicotinamide (NAM), which blocks deacetylase and mono-ADP-ribosylase activities of SIRT6. NAM altered the size of G3BP granules in a similar manner as the absence of SIRT6 (Fig. 6B,C). The analysis of G3BP::GFP expression at the cellular level by immunoblotting verified that the exogenous G3BP::GFP was expressed at a similar level in SIRT6KO MEFs, wild-type MEFs and MEFs treated with NAM (Fig. 6D).

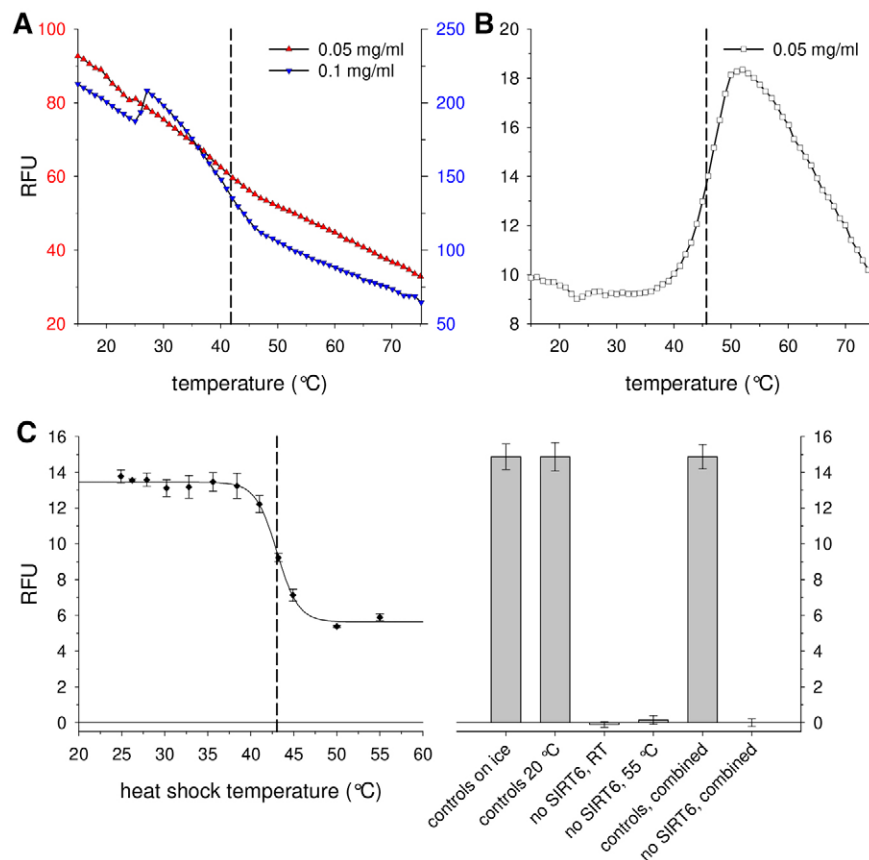


**Fig. 5. Thermostability and thermoactivity of human recombinant SIRT6.** The thermal stability of SIRT6 was analyzed using intrinsic tryptophan fluorescence (A) and differential scanning fluorimetry, where the fluorescent dye Sypro Orange was used to detect hydrophobicity changes in the protein solution (B). Owing to the relatively weak change in relative fluorescence units (RFU) during the temperature ramp, intrinsic fluorescence experiments were also performed using a protein concentration of 0.1 mg/ml. To determine a SIRT6 thermoactivity profile, deacetylation of a labeled human p53 peptide was monitored after heat shock at various temperatures (C). Error bars represent the s.d. of triplicate samples. Signals of control samples are shown on the right (same scale; RT, room temperature). In all three panels, dotted lines indicate deduced transition midpoints according to a two-state model, which were  $41.8^\circ\text{C}$  (A),  $45.7^\circ\text{C}$  (B) and  $43.0^\circ\text{C}$  (C).

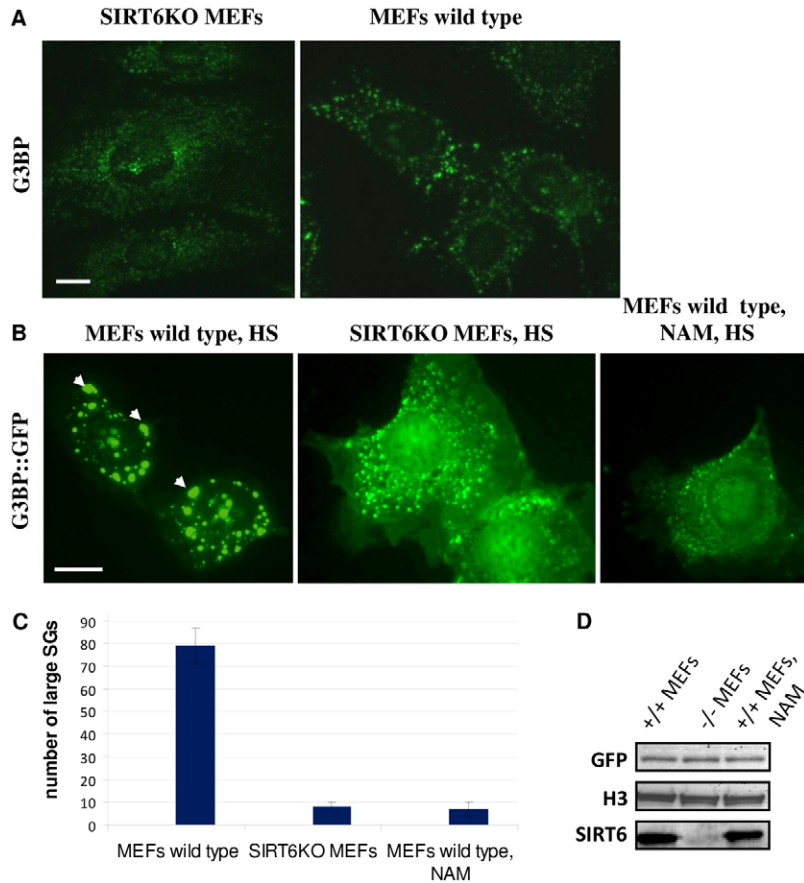


**Fig. 6. SIRT6 impacts G3BP assembly.** (A) Representative images of wild-type MEFs and SIRT6KO MEFs in heat-shock condition. Stress granules were detected by antibody raised against G3BP. Scale bar: 10  $\mu$ m. (B) Wild-type MEFs (with or without NAM treatment) and SIRT6KO MEFs transfected with G3BP::GFP and analyzed for heat-shock-induced stress granule formation. Arrowheads indicate large stress granules. Scale bars: 10  $\mu$ m. (C) The graph shows the average size of G3BP::GFP granules in MEFs. Analysis was based on 50 transfected cells. The large class of granules was identified on the basis of size (large, 31–230 pixels<sup>2</sup>). Results shown are mean values of three independent experiments. Results are means  $\pm$  s.d. (D) The cellular level of G3BP::GFP in cells used in B. H3 served as a loading control.

To determine whether deacetylase or mono-ADP-ribosylase activities of SIRT6 are required for SIRT6-dependent assembly of stress granules, we overexpressed several SIRT6 deletion mutants in stressed and non-stressed NIH3T3 cells. Analysis of various point mutations that disrupt either the deacetylase (H133Y, R65A) or the mono-ADP-ribosyltransferase activity (S56YG60A) of SIRT6 revealed that the deacetylase activity and especially the His133 residue is important for G3BP granule formation (supplementary material Figs S8, S9). Similarly, the ability of *C. elegans* SIR-2.4 to induce stress granule formation in the NIH3T3 cell line also depended on its deacetylase activity (data not shown), indicating that the evolutionary conserved mechanism that regulates formation of G3BP-containing stress granules requires the deacetylase activity of SIRT6.

To provide more evidence that the deacetylase activity of SIRT6 is important for stress granule formation, we attempted to rescue SIRT6KO MEF cells with wild-type SIRT6::GFP and mutated SIRT6H133Y::GFP fusion proteins. We observed that the restoration of wild-type SIRT6 levels by expression of SIRT6::GFP rescued the number of large stress granules (Fig. 7A,B). Importantly, the enzymatically-inactive SIRT6H133Y::GFP failed to efficiently rescue the number of stress granules in SIRT6KO MEFs, suggesting that the deacetylase activity of SIRT6 is necessary to regulate the formation of stress granules (Fig. 7A,B). The analysis of SIRT6::GFP and SIRT6H133Y::GFP expression at the cellular level by immunoblotting of the transfected SIRT6KO MEFs verified that the exogenous SIRT6::GFP and SIRT6H133Y::GFP constructs were both expressed at similar levels (Fig. 7C).

#### SIRT6 does not influence the acetylation status of G3BP

Because G3BP is acetylated at Lys376 (Choudhary et al., 2009), we wanted to determine whether SIRT6 controls assembly of stress granules by deacetylation of G3BP; we therefore analyzed the acetylation status of G3BP under different conditions by mass spectrometry. However, neither the absence of SIRT6 nor the inhibition of SIRT6 by NAM affected acetylation of G3BP (supplementary material Fig. S10A). In addition, use of the acetylation-deficient mutant of G3BP yielded stress granules of similar sizes and in similar numbers as wild-type G3BP (supplementary material Fig. S10B), indicating that assembly of stress granules does not depend on the acetylation status of G3BP.

#### SIRT6 influences phosphorylation of G3BP at Ser149

Next, we examined whether the absence of SIRT6 affects phosphorylation of G3BP at Ser149, which has been shown to inhibit stress granule assembly after arsenite treatment and heat shock (Tourrière et al., 2003). Strikingly, SIRT6-deficient MEFs showed increased phosphorylation of G3BP<sub>Ser149</sub> under physiological and heat-shock conditions (Fig. 7D). Addition of the SIRT6 inhibitor NAM to wild-type MEFs also increased phosphorylation of G3BP<sub>Ser149</sub>, whereas NAM had little effect in SIRT6KO MEFs (Fig. 7D). Because our data indicate that deacetylase activity of SIRT6 is important for induction of G3BP foci, we asked whether it also affects G3BP phosphorylation. Therefore, we analyzed the phosphorylation status of G3BP at Ser149 in SIRT6KO MEFs after overexpression of wild-type and

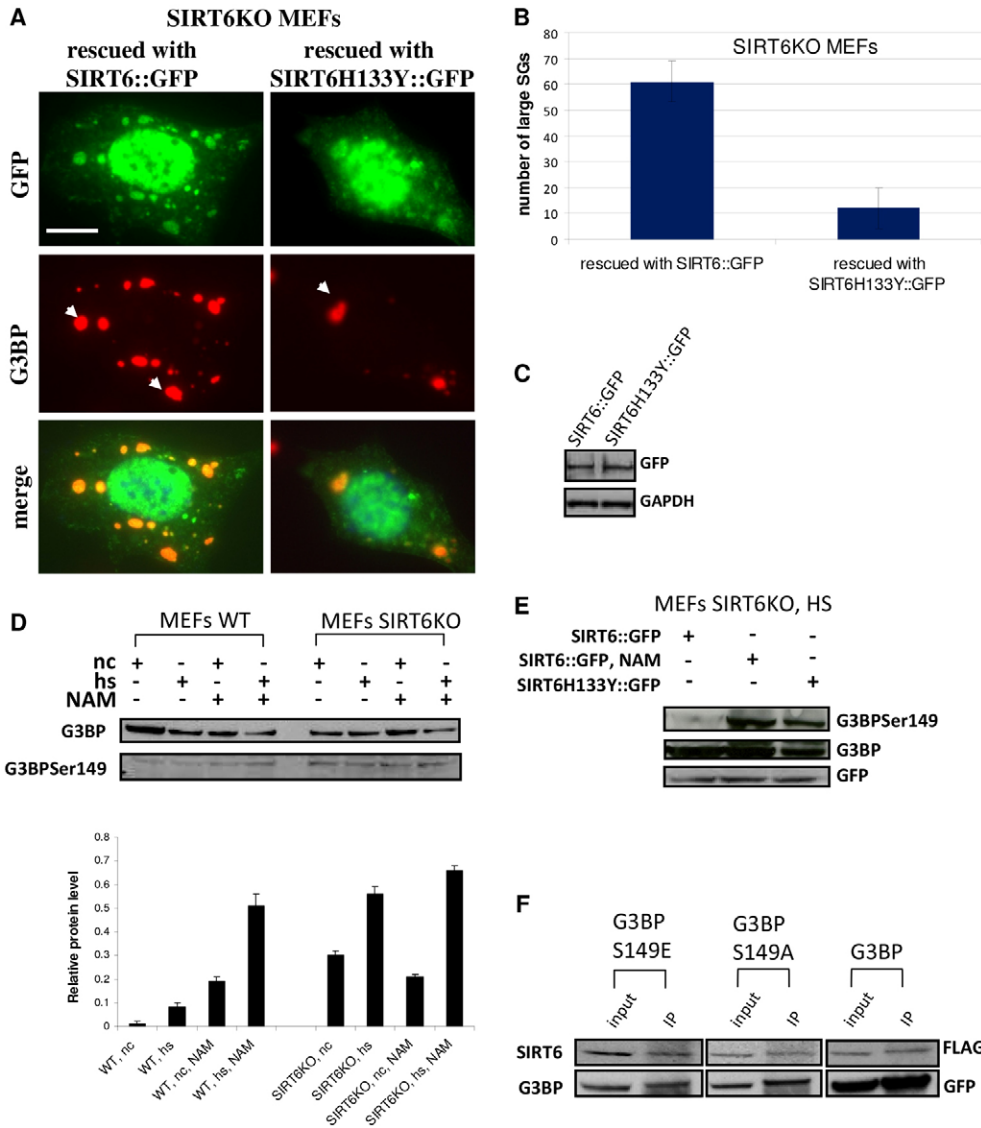


**Fig. 7. Deacetylase activity of SIRT6 influences stress granule assembly and the level of G3BP phosphorylation.**

(A) SIRT6::GFP but not SIRT6H133Y::GFP expression in SIRT6KO MEFs restores the number of large stress granules (arrowheads). Scale bar: 10  $\mu$ m. (B) Quantification of the number of large stress granules based on size (large, 31–230 pixels<sup>2</sup>). Analysis was based on 50 transfected cells (two independent experiments; means  $\pm$  s.d.) (C) The exogenous, mutated form of SIRT6H133Y::GFP is expressed at comparable level to the SIRT6::GFP wild-type form. (D) Phosphorylation level of G3BP in non-stressed and heat-shock-stressed wild-type and SIRT6KO MEFs with or without NAM treatment. nc, normal condition; hs, heat-shock condition. Bar graph for the quantitative comparison among protein expression level is shown below. The signal intensity of a protein band and its surrounding background were scanned from images derived from two independent western blot experiments for each protein and quantified by using Scanalytics IPLAB 3.6 (Rockville, MD). The resultant background-subtracted values of G3BPSer149 were normalized to those of G3BP and then plotted as the relative protein levels for each protein at each condition in each cell line with or without NAM treatment. (E) Phosphorylation level of G3BP in stressed SIRT6KO MEFs cells rescued with SIRT6 wild-type and SIRT6-mutated form. MEFs sorted by FACS were used for western blot analysis. (F) Western blot analysis showing co-immunoprecipitation of FLAG-tagged SIRT6 and GFP-tagged wild-type G3BP and G3BP carrying point mutations of the phosphorylation site (S149E or S149A).

catalytically inactive form of SIRT6::GFP fusion protein (Fig. 7E). Although overexpression of wild-type SIRT6 in SIRT6KO MEFs decreased G3BPSer149 phosphorylation, addition of the SIRT6 inhibitor NAM abolished this effect. This indicates that the deacetylase activity of SIRT6 is important for both G3BP foci formation and its de-phosphorylation at Ser149. The phosphorylation status of G3BP at Ser149 did not affect the association of SIRT6 and G3BP because both the phosphorylation-mimetic (S149E) and the phosphorylation-deficient (S149A) G3BP mutants interacted to the same extent as wild-type G3BP with SIRT6 in NIH3T3 cells (Fig. 7F). Similarly, the catalytic activity of SIRT6 was dispensable for the interaction of SIRT6 with G3BP, as indicated by efficient coimmunoprecipitation of G3BP with the acetylase-deficient SIRT6H133Y mutant (supplementary material Fig. S11).

#### SIRT6 affects disassembly of stress granules

To assess whether SIRT6 affects disassembly of stress granules during stress recovery, we examined the size of G3BP::GFP foci at various time points after release from heat shock. We observed that the SIRT6KO MEFs recovered poorly after stress release when

compared with wild-type cells, indicating that SIRT6 also promotes G3BP disassembly after stress (Fig. 8A; supplementary material Fig. S12). Interestingly, the disaggregation of stress granules after removal of the stressor is important for the recovery of cellular functions after stress and shows age-related changes (Gallouzi, 2009).

#### SIRT6 increases cell survival

Because sequestration of highly expressed mRNAs and proteins in stress granules enhances cell viability (Lavut and Raveh, 2012), we examined whether impaired stress granule formation in SIRT6KO MEFs correlates with lower cell survival. In fact, SIRT6KO MEFs showed strongly decreased viability (ca. 30%) compared with wild-type cells under stress and non-stressed conditions (Fig. 8B). A decreased cell viability of SIRT6KO MEFs reflects a conserved role of mammalian SIRT6 and SIR-2.4 in *C. elegans* in preserving cell survival. The enzymatic activity of SIRT6 is important for efficient stress granule induction and for inhibition of G3BPSer149 phosphorylation; we therefore analyzed whether transfection of wild-type SIRT6 and its catalytic mutant differentially affect survival of SIRT6KO

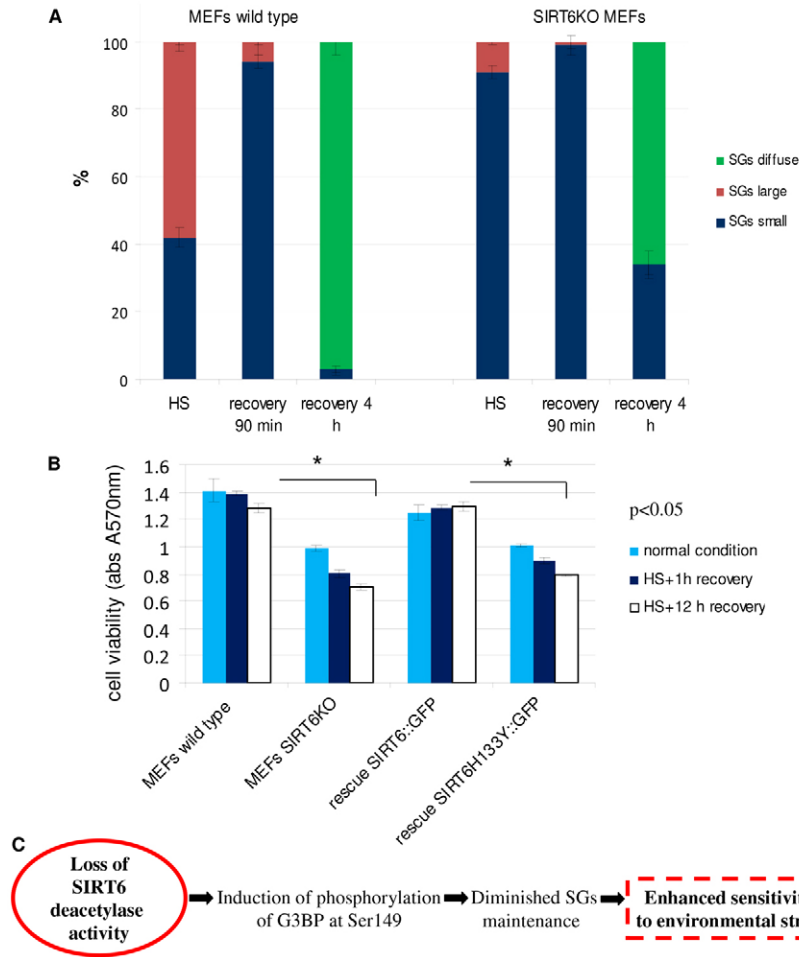


**Fig. 8. SIRT6 deficiency impacts disassembly of stress granules and influences cell viability.** (A) Size of G3BP foci after heat shock release. SIRT6<sup>+/+</sup> and SIRT6<sup>-/-</sup> cells heat-shocked for 30 minutes were then incubated for 90 minutes or 4 hours at 37°C (recovery). The size of G3BP::GFP granules were analyzed directly after heat shock and after 90 minutes or 4 hours of recovery at 37°C ( $n=100$  cells in ten random fields, quantification as a percentage, means  $\pm$  s.d.). The two classes of granules were identified on the basis of size (small, 1–30 pixels<sup>2</sup>; large, 31–230 pixels<sup>2</sup>). (B) MTT assay demonstrating an increased viability of SIRT6KO MEFs after transfection with SIRT6::GFP but not with SIRT6H133Y::GFP (results shown are mean  $\pm$  s.d. of two independent experiments; \* $P<0.05$  versus wild-type MEFs or SIRT6KO MEFs rescued with SIRT6::GFP or SIRT6H133Y::GFP, respectively). (C) Hypothetical working model.

MEFs. Indeed, we were able to detect increased survival of SIRT6KO MEFs cells expressing wild-type SIRT6, but not mutated SIRT6 (Fig. 8B).

Taken together, our data suggest that SIRT6 deacetylase activity regulates assembly and disassembly of stress granules, probably by promoting dephosphorylation of G3BP at Ser149. Reduced formation of stress granules and delayed recovery after stress will enhance sensitivity to environmental stressors in cells lacking SIRT6 or in *sir-2.4* mutant animals (Fig. 8C).

## Discussion

We have shown that SIRT6 is not only a chromatin-associated protein and a regulator of transcription factors, histones and PARP activities, but also translocates into the cytoplasm upon stress, interacts with G3BP and regulates stress granule assembly and disassembly (Michishita et al., 2008; Michishita et al., 2009; McCord et al., 2009; Kawahara et al., 2009; Mao et al., 2011). Although SIRT6 is found almost exclusively in the nucleus (Mostoslavsky et al., 2006; Kawahara et al., 2009; Tennen et al., 2010), some fraction of SIRT6 is present in secretory organelles, such as the endoplasmic reticulum (Jiang et al., 2013). In *C. elegans*, we observed binding of SIR-2.4 to structures located near the nucleoplasmic side of the nuclear envelope, suggesting that the intranuclear SIR-2.4 plays an important role in this structure. Our data using mammalian cell cultures showed clearly that the cytoplasmic SIRT6 fraction participates in the formation of stress granules, despite the fact that

the SIRT6 protein contains a functionally active nuclear localization signal (NLS) (Tennen et al., 2010). We propose that the shift in the nuclear and cytoplasmic distribution of SIRT6 upon stress might be accompanied by binding to G3BP and/or SIRT6 protein stability changes, which modify the secondary structure in a way that leads to masking of the NLS. This speculation is consistent with our biophysical data showing that human recombinant SIRT6 is functional at 37°C and changes its stability above a temperature of 40°C. We cannot exclude the possibility that at temperature stress conditions *in vivo*, SIRT6 is misfolded and/or degraded by proteasomes. However, it is also conceivable that misfolded SIRT6 protein escapes degradation as a result of interactions with heat-shock proteins such as HSP-70 (M.J.B., unpublished results). Consistent with this idea, we showed in cell culture that SIRT6 protein manifests functionality by enhanced viability of the rescued SIRT6 KO MEFs after heat-shock recovery (Fig. 8B).

Our data indicate that SIRT6 indirectly regulates dephosphorylation of G3BP Ser149, which is an important step during stress granule formation. The exact mechanism by which SIRT6 mediates G3BP dephosphorylation at Ser149 is unknown and requires further investigation. G3BP Ser149 is phosphorylated in a p120RasGAP-dependent manner, but the mechanism by which RasGAP maintains phosphorylation has not been explored (Parker et al., 1996; Gallouzi et al., 1998; Tourrière et al., 2001). It seems likely that SIRT6 deacetylates and regulates components of the enzymatic machinery that controls the phosphorylation status of

G3BPSer149. A similar feedback loop has been described for the regulation of eIF2- $\alpha$  phosphorylation by SIRT1 (Ghosh et al., 2011). Because loss of SIRT6 did not completely abrogate formation of G3BP foci after heat shock, we assume that SIRT6 is not the only important factor that regulates phosphorylation of G3BP. Stress granules contain large numbers of post-translationally modified proteins that affect assembly of granules (Ohn and Anderson, 2010). Currently, we cannot exclude the possibility that SIRT6 modifies additional proteins in the stress granule multiprotein complex and therefore impacts stress granule assembly by other mechanisms. Our results clearly document that SIRT6 is instrumental for rapid stress responses not only in the nuclear but also in the cytoplasmic compartment.

The enzymatic activity of SIRT6 offers quick, economical and reversible means to adjust protein function during stress, analogous to the histone deacetylase protein 6 (HDAC-6) (Kwon et al., 2007; Kawaguchi et al., 2003). Our results reveal that the role of SIRT6 in cytoplasmic stress granule formation is remarkably conserved during evolution. Because assembly of stress granules in response to stress and efficient disassembly during stress recovery are both important prosurvival mechanisms that are impaired during aging (Gallouzi, 2009), it is tempting to speculate that SIRT6 affects age-related processes not only in the nucleus but also in the cytoplasm by regulating the structure and dynamics of stress granules. The redistribution of nuclear SIRT6 to cytoplasmic stress granules potentially reveals new connections between protein deacetylation and global gene expression control. Future studies with regard to detailed mechanistic insights of how SIRT6 is able to promote dephosphorylation of G3BP are needed to provide a clearer understanding of how SIRT6 is able to regulate the formation of stress granules.

## Materials and Methods

### Trp fluorescence transition

Human recombinant SIRT6 (1–355 amino acids, N-terminally (His)<sub>6</sub>-tagged) was obtained from Cayman Chemical (Ann Arbor, MI). The supplied 0.6 mg/ml protein solution in 25 mM Tris-HCl, 100 mM NaCl, 20% glycerol, pH 8, was diluted to 0.05 or 0.1 mg/ml SIRT6, respectively, using buffer without glycerol. Intrinsic tryptophan fluorescence intensity was monitored at a temperature ramp rate of 1°C/minute using a FP-6500 spectrofluorometer (Jasco, Germany) equipped with an ETC-273T Peltier device. Quartz cuvettes with a path length of 1 cm were used. The excitation wavelength was set to 280±3 nm and fluorescence emission was recorded at 341±5 nm. Under the assumption of a two-state transition, nonlinear least-squares fitting was performed using SigmaPlot 12 (Systat Software) in order to determine apparent midpoints of thermal unfolding. Linear pre- and post-transition baseline corrections were applied as described (Allen and Pielak, 1998). The signal of buffer solution without SIRT6 was <6 RFU (data not shown).

### Differential scanning fluorimetry

Human recombinant SIRT6 was probed for thermal stability in the presence of the fluorescent dye Sypro Orange (Life Technologies). Similar to solutions containing substances such as 1-anilinoanthracene-8-sulfonic acid (ANS), this dye can exhibit marked changes in its fluorescence properties upon protein unfolding (Lavinder et al., 2009). Solutions contained 0.05 mg/ml protein and a dye concentration of 5 $\times$  (relative to the supplied stock, absolute dye concentrations are not disclosed by the manufacturer). Using the same equipment as above, dye fluorescence upon excitation at 470 nm (3 nm bandwidth) was monitored at 563 nm (10 nm bandwidth) during a temperature ramp of 1°C/minute. In the absence of SIRT6, the signal of Sypro Orange in buffer was 1.43±0.03 RFU over the temperature range tested (data not shown).

### Temperature dependence of SIRT6 activity

SIRT6 Direct Fluorescent Screening Assay Kit (Cayman Chemical, Ann Arbor, MI) was used to determine the temperature dependence of human recombinant SIRT6 deacetylase activity. Unless stated otherwise, experimental steps were performed as recommended by the manufacturer and by using the supplied solutions. SIRT6 was mixed with assay buffer prepared with glass-distilled water to yield samples of 35  $\mu$ l. Transferred into 0.2 ml thin-wall PCR tubes, triplicate samples were incubated for

10 minutes at various temperatures and subsequently brought to 20°C using PCR thermocyclers (peqSTAR 2X, Peqlab, Germany; Mastercycler personal and gradient, both Eppendorf, Germany). Control reactions were incubated on ice. Subsequently, 15  $\mu$ l substrate solution containing NAD<sup>+</sup> and aminomethylcoumarin-labeled human p53 peptide [Arg-His-Lys-Lys( $\epsilon$ -acetyl)-AMC] was added to each sample. After 1 hour of incubation at 37°C on a shaker, 50  $\mu$ l Stop/Developer solution containing nicotinamide was added, followed by 30 minutes of incubation at room temperature. Individual samples were transferred into black 96-well half area black flat bottom polystyrene NBS plates (Corning). Fluorescence intensity upon excitation at 360 nm was measured at 460 nm using a SkanIT Varioskan Flash plate reader (Thermo Scientific). Bandwidth and measurement time were set to 5 nm and 200 milliseconds, respectively. The relative fluorescence signal of substrate solution in buffer without SIRT6 (mean of room temperature and 55°C) was subtracted from all samples.

### Cell lines and transfection

NIH3T3, U2OS, SIRT6 knockout (SIRT6<sup>-/-</sup>), G3BP knockout (G3BP<sup>-/-</sup>) and wild type (SIRT6<sup>+/+</sup> or G3BP<sup>+/+</sup>) MEFs were maintained in Dulbecco's modified Eagle's medium (DMEM) with 10% fetal bovine serum, and grown at 37°C in 5% CO<sub>2</sub>. Transfections were performed with FuGENE HD Transfection Reagent (Roche) following the manufacturer's protocol. Cells were transfected with following constructs: SIRT1::YFP, SIRT1::CFP, SIRT6::YFP, SIRT6::GFP, SIRT6H133Y::GFP, SIRT6R65A::GFP, SIRT6S56YG60A::GFP, SIRT6::CFP, SIRT6::FLAG, SIRT7::CFP, G3BP::GFP, G3BP::FLAG, G3BPS149E::GFP, G3BPA149A::GFP, SIR-2.4::GFP or K08F4.2::RFP. SIRT6 domains in pEGFP-N2-FLAG backbone have been described previously (Tennen et al., 2010). For stress granule formation, cells were heat shocked (20 minutes, 30 minutes or 1 hour at 42°C) or incubated with sodium arsenite (1 hour, 1 mM). Cycloheximide (Sigma-Aldrich, Germany) was used at 10  $\mu$ g/ml. The infected MEF cells were expanded and sorted by FACS. GFP-positive cells were used for experiments.

### MTT assay

Cells were allowed to recover from that point on for periods of 90 minutes or 4 hours. Cell viability was determined using MTT assays. For the MTT assay, PBS containing 5 mg/ml MTT was added to cells. Cells were incubated for 2 hours in the absence of light. The medium was removed, and precipitates were resuspended in 50  $\mu$ l DMSO. Absorbance at 570 nm was measured using a plate reader. Experiments were performed in triplicate.

### C. elegans strains

*C. elegans* strains were grown at 15°C or 20°C. The wild-type strain was the N2 (Bristol) strain. The following mutant alleles and strains were used: *rrf-1(pk1417)* and *mpgEx16[sir-2.4pr::sir-2.4::gfp rol-6(su1006)]*, translational fusion. For feeding, the F1 generation was grown at 15°C and L4 larvae were transferred on pre-warmed NGM plates and incubated at 25°C. Three-day-old hermaphrodites were transferred from 25°C on new pre-warmed plates and incubated at 36.5°C for the next 12 hours.

### Generation of *sir-2.4::gfp* transgenic strain

The reporter *sir-2.4* gene construct with promoter was generated by a PCR from cosmid C06A5 (The Sanger Centre, Cambridge, UK) using the primers GGAAATCCGGGATCAAGGCTCGTGAGTT (with *EcoRI* cut site) and CGGGATCCAAACGTCAGCATGAATTGCAG (with *BamHI* cut site). The PCR product was inserted into pEGFP-N1 (Clontech). For the cloning into pPD118.25 vector (Addgene), *sir-2.4* cDNA was amplified using following primer pair: CCGGATCCATCCATATGACGTCCACAGCATGCCATGAAATCTGCAAAATACAAAACCG (with *BamHI* cut site) and ATAAGATGCGG-CCGCGCTAATTTTCAATGGAATAGGCAC (with *NotI* cut site). To generate *sir-2.4* transgenic worms, 25 ng/ $\mu$ l or 10 ng/ $\mu$ l of the plasmid together with 75 ng/ $\mu$ l or 90 ng/ $\mu$ l pRF4 plasmid carrying the dominant mutant *rol-6(su1006)* were injected into wild-type worms according to published methods (Mello et al., 1991). Transgenic worms displaying a roller phenotype were analyzed for GFP expression. For the visualization of GFP fluorescence in live animals, worms were transferred to a 10  $\mu$ l drop of 2 mM NaN<sub>3</sub> and mounted directly onto agarose (2%) pads.

### Generation of cDNA encoding *sir-2.4* or K08F4.2

A cDNA encoding *sir-2.4* was cloned into pET3a vector (Invitrogen) or L4440 vector (Addgene) after RT-PCR amplification from total RNA of wild-type *C. elegans* using Superscript II polymerase (Promega) according to the manufacturer's instructions. For the procedure, the following primer pair was used: *sir-2.4* cDNA forward primer, ATGAAATCTGCAAAATACAAAACCG and *sir-2.4* cDNA reverse primer, TTAGCTAATTTTCAATGGAATAGGCAC. A cDNA of the K08F4.2 gene was identified using the Wormbase Website (<http://www.wormbase.org>) and amplified by RT-PCR. K08F4.2 cDNA was cloned into pmCherry-N1 (Addgene) and used for co-transfection.

### RNA interference by feeding

In short, the feeding construct L4440-*sir-2.4* (cDNA) was transformed into *E. coli* strain HT115 (DE3). 50  $\mu$ l of the bacterial culture incubated overnight at 37°C

with constant shaking were spread on 40 mm NGM feeding plates containing 100 µg/ml ampicillin and 1 mM IPTG. Finally, plates were incubated 8 hours at room temperature to grow a bacterial lawn and to induce dsRNA. Two hermaphrodites in L3-larval stages were transferred on the plate and incubated 24 hours at 25°C. Every 12 or 24 hours, the hermaphrodites were transferred to fresh feeding plates. The F1 generation as 3-day-old hermaphrodites was used for the thermotolerance assay and immunostaining.

#### Thermotolerance assay

A total of 40 3-day-old hermaphrodites (in three independent experiments) were transferred on pre-warmed NGM plates and incubated at 36.5°C for 12 hours. The survival was scored every hour at 36.5°C as the number of animals that showed touch-provoked movement. Animals that failed to display motility or pharyngeal pumping were scored as dead.

#### Measurements of P granules number

P granules of 20 nuclei of pachytene-stage germline cells were counted manually along Z-stack images for each genotype. The experiment was repeated three times.

#### Treatment with inhibitors

Transfected or co-transfected cells were treated with NAM inhibitor (final concentration 5 mM, Sigma-Aldrich) and incubated for 16 hours.

#### Antibodies

The following antibodies were used in the study: anti-G3BP (ab56574), anti-G3BPSer149 (Sigma, G8046), anti-H3 (ab1791), anti-PABP (ab21060), anti-FLAG (M2, Sigma F1804), anti-GFP (clone 7.1 and 13.1 Roche), anti-GFP (ab6556), anti-GAPDH (Pierce, MA1-22670), mouse monoclonal anti-PGL-1/PGL-3 KT3 (Hybridoma Bank, University of Iowa), anti-GLH-1.2 (kindly provided by Ch. Eckmann, Dresden), anti-tudorSN (sc-67128), anti-TIAL-1 (ab26257), anti- $\alpha$ -tubulin (1:5000, Sigma), anti-SIRT6 (ab62739), anti-SIRT6 (Cell Signaling, 2590); anti-SIRT2 (ab32829), anti-acetylK (Cell Signaling, 9441), anti-NPC(mAb414, ab24609) or anti-RFP (Chromotek, 5F8). For the immunostaining procedure, the following secondary antibodies were used: Alexa Fluor 568 goat anti-mouse (Life technologies, A-21124), Alexa Fluor 555 goat anti-rabbit (Life technologies, A-21428), DyLight 488 anti-mouse (Thermo Scientific, 35503) or DyLight 488 anti-rabbit (Thermo Scientific, 35553).

#### Generation of antibody against SIR-2.4

The synthetic peptide SIR-2.4 (CHEKIVETAIHADVKL) was chemically synthesized and coupled with sulfo-maleimidobenzoyl-*N*-hydroxysuccinimide ester (WITA) to BSA. 500 mg of antigen were used for rabbit immunization in a series of three injections. Antigen injections and resulting antiserum collections were performed by SEMBID (Slovakia). Anti-SIR-2.4 antibody was affinity purified with a SulfoLink (Pierce) column using 1 mg of the synthetic peptide. The specificity was tested on western blot. In addition, to confirm that the observed SIR-2.4 signal is a result of the interaction of the antibody with target antigen instead of non-specific binding, pre-absorption with the blocking peptides was performed. For preabsorption, SIR-2.4 antibody (diluted 1:80) was incubated with 1 µg peptide for 1 hour at room temperature before incubation with *C. elegans* tissues.

#### Immunostaining of *C. elegans*

Worms from wild-type strain were fixed in 1% PFA (for staining using anti PGL-1/-3) or with methanol and acetone (for anti-GLH-1.2 staining) and stained, as previously described (Jedrúsik and Schulze, 2007).

#### Immunostaining of cells

For each immunofluorescence analysis, cells were seeded in Lab-TekII Chamber Slides (ThermoFisher), transfected or co-transfected with plasmid of interest and incubated for 24 hours at 37°C. Cells were then washed with DPBS (Gibco), incubated with 4% PFA for 15 minutes at room temperature. Next, cells were washed three times for 5 minutes with DPBS and incubated for 15 minutes in 0.1% TritonX-100 diluted in DPBS. Finally, cells were blocked with 5% BSA in DPBS for 1 hour and incubated with first antibody for 1 hour at room temperature. After incubation, chamber slides were washed three times for 5 minutes in DPBS and incubated with secondary antibody followed by DAPI counterstaining. After final washing, the cells were closed with Vectashield mounting medium and analyzed using Leica DMI 6000B fluorescence microscope.

#### Immunoprecipitation

For each experiment, NIH3T3 cells were seeded in 10 cm culture dishes, transiently co-transfected with the plasmid of interest. Before harvesting, cells were washed twice with 5 ml of ice-cold PBS buffer and incubated for 2 minutes with 300 µl NP40 lysis buffer containing Complete, EDTA-free, Protease Inhibitor Cocktail tablet (Roche). Next, cells were scraped using a cold plastic cell scraper and the cell suspension was transferred and then incubated on a rotator for 30 minutes at 4°C with constant

rotation. After centrifugation (15 minutes at 13,000 rpm) each supernatant was transferred into a new 1.5 ml tube and incubated with an antibody or without (IgG negative control) overnight at 4°C with constant rotation [Optional-for RNase A control, supernatant was treated with 100 µg/ml RNase A (Qiagen) before adjusting the antibody]. In addition, the cell suspension was used for RNA isolation (PureLink RNA Mini Kit, Ambion) and RNase treatment to demonstrate the integrity of the rRNA on agarose gel. On the following day, 80 µl slurry of the Pierce Protein-G agarose beads or antibody were added to cell lysates and incubated for 2 hours at 4°C with constant rotation. For immunoprecipitation using RFP-tagged proteins, 50 µl of RFP-TrapA slurry (Chromotek, Germany) was used. After incubation, lysates were centrifuged for 2 minutes at 2800 rpm at 4°C, the supernatants were discarded and the beads washed three times with fresh NP40 lysis buffer containing Complete, EDTA-free, Protease Inhibitor Cocktail tablet (Roche). The beads were mixed with 4× LDS sample buffer, 10× reducing agent and boiled for 5 minutes, and briefly centrifuged at 13,000 rpm. The supernatants were loaded on NuPage 4–12% Bis-Tris Gel 1.0 mm × 10 wells and run using NuPage4-MOPS SDS Running Buffer (20×). For co-immunoprecipitation, the following *in vitro* translated proteins were used: G3BP (Abnova, H00010146) expressed in wheat germ expression system, PABP (ab92269) and SIRT6 (Active Motif, 31336). These proteins were combined and incubated at 30°C for 30 minutes. Co-immunoprecipitation was performed at 4°C for 2 hours with 3 µl anti-G3BP or SIRT6-antibody-coupled resin. IgG (sample without antibody) was used as a negative control. Eluted proteins were resolved using 4–20% SDS-PAGE and visualized by autoradiography.

#### Fractionation

NIH3T3 cells were transfected as described above and subjected to nuclear and cytoplasmic extraction as previously described (Dignam et al., 1983).

#### Quantification of cells containing stress granules and measurement of stress granule size

For quantification, ten fields of each sample were randomly selected. The percentage of cells containing stress granules was counted. For measurement of the size of stress granules, 10 cells of each sample were randomly selected and the relative size (pixels<sup>2</sup>) was determined from selected images taken at 40× magnification using Leica DMI 6000B fluorescence microscope. Granules were defined using the threshold function in ImageJ (<http://rsb.info.nih.gov/ij>) according to previously described procedure (Dolzanskaya et al., 2011). The data were imported into Excel for subsequent analysis. The average stress granule size of at least 100 stress granules in 10 cells was presented. The number of stress granules in each experiment was calculated using ten random fields each containing 10–20 cells. Data are represented as the means of three experiments ± s.d. (error bars).

#### Yeast two-hybrid screen

The yeast strain AH109 was used for all yeast two-hybrid experiments. The full-length cDNA of *sir-2.4* was cloned in pGBKT7 and pGADT7 (Clontech). An autoactivation test with these two vectors was negative. The *sir-2.4* cDNA in pGBKT7 as prey was used to screen a *C. elegans* cDNA library in the corresponding bait vector. Transformants were selected on SD plates without Trp, Leu and His. In total about 2×10<sup>6</sup> transformants were screened. Positive clones were retested and then sequenced.

#### Mass spectrometry analysis

Cells were transfected to express GFP-Sirt6, followed by immunoprecipitation with anti-GFP antibody. Gel bands were excised and subjected to in-gel digestion with trypsin (Shevchenko et al., 2006). The resulting tryptic peptides were extracted with acetonitrile and desalted with reverse-phase C18 STAGE tips (Rappsilber et al., 2007). Mass spectrometric experiments were performed on a nano-flow HPLC system (Proxeon) connected to LTQorbitrap and Velos LTQ-Orbitrap-XL instruments (Thermo Fisher Scientific) equipped with a nano-electrospray source (Proxeon) (Drexler et al., 2012). The RAW files were analyzed with the MaxQuant software tool (Version 14.10) (Cox and Mann, 2008).

#### Statistical analysis

Data were analyzed by Student's *t*-test. Statistical analyses of lifespan were performed on Kaplan–Meier survival curves in GraphPad Prism 5 by log-rank tests. To compare the interaction between genotype and RNAi, two-way ANOVA tests were used.

#### Acknowledgements

We are especially grateful to Katrin Chua (Stanford University) for the SIRT6 construct plasmids, Christian Eckmann (MPI, Dresden) for the antibody against GLH-1.2 and Toni Gartner (Dundee University) for anti-SIR-2.1. We thank M. Euler for technical assistance. Some *C. elegans* strains used were obtained from the Caenorhabditis Genetics Center (CGC), which is funded by the NIH National Center for Research Resources (NCR).

## Author contributions

M.J.-B. conceived the study, made contributions to the concept and design of the manuscript; M.J.B. and E.B. designed the experiments; M.J.-B., M.S., C.S., H.S., J.K., F.P., T.B., S.M. and M.K. performed and analyzed the data; J.T., K.M.M. and T.B. contributed reagents and materials; M.-J.B. wrote the first draft of the manuscript; E.B. and T.B. edited the manuscript.

## Funding

This work was supported by the German National Funding Agency (DFG) [grant number JE 505/1-3 to M.J.-B.]; and the Max Planck Society (M.J.-B.). J.T. and S.M. are supported by the Fondation pour la Recherche Médicale (FRM) [grant number Equipe FRM 2011–n°DEQ20111223745]. Deposited in PMC for immediate release.

Supplementary material available online at

<http://jcs.biologists.org/lookup/suppl/doi:10.1242/jcs.130708/-/DC1>

## References

- Allen, D. L. and Pielak, G. J. (1998). Baseline length and automated fitting of denaturation data. *Protein Sci.* **7**, 1262–1263.
- Anderson, P. and Kedersha, N. (2006). RNA granules. *J. Cell Biol.* **172**, 803–808.
- Anderson, P. and Kedersha, N. (2009). Stress granules. *Curr. Biol.* **19**, R397–R398.
- Buchan, J. R. and Parker, R. (2009). Eukaryotic stress granules: the ins and outs of translation. *Mol. Cell* **36**, 932–941.
- Chiang, W.-C., Tishkoff, D. X., Yang, B., Wilson-Grady, J., Yu, X., Mazer, T., Eckersdorff, M., Gygi, S. P., Lombard, D. B. and Hsu, A.-L. (2012). *C. elegans* SIRT6/7 homolog SIR-2.4 promotes DAF-16 relocalization and function during stress. *PLoS Genet.* **8**, e1002948.
- Choudhary, C., Kumar, C., Gnad, F., Nielsen, M. L., Rehman, M., Walther, T. C., Olsen, J. V. and Mann, M. (2009). Lysine acetylation targets protein complexes and co-regulates major cellular functions. *Science* **325**, 834–840.
- Cox, J. and Mann, M. (2008). MaxQuant enables high peptide identification rates, individualized p.p.b.-range mass accuracies and proteome-wide protein quantification. *Nat. Biotechnol.* **26**, 1367–1372.
- Dignam, J. D., Lebovitz, R. M. and Roeder, R. G. (1983). Accurate transcription initiation by RNA polymerase II in a soluble extract from isolated mammalian nuclei. *Nucleic Acids Res.* **11**, 1475–1489.
- Dolzhanakaya, N., Xie, W., Merz, G. and Denman, R. B. (2011). EGFP-FMRP forms proto-stress granules: A poor surrogate for endogenous FMRP. *J. Biophys. Struct. Biol.* **3**, 1–23.
- Drexler, H. C., Ruhs, A., Konzer, A., Mandler, L., Bruckskotten, M., Looso, M., Günther, S., Boettger, T., Krüger, M. and Braun, T. (2012). On marathons and Sprints: an integrated quantitative proteomics and transcriptomics analysis of differences between slow and fast muscle fibers. *Mol. Cell. Proteomics* **11**, M111.010801.
- Gallouzi, I. E. (2009). Could stress granules be involved in age-related diseases? *Aging* **1**, 753–757.
- Gallouzi, I. E., Parker, F., Chebli, K., Maurier, F., Labourier, E., Barlat, I., Capony, J. P., Tocque, B. and Tazi, J. (1998). A novel phosphorylation-dependent RNase activity of GAP-SH3 binding protein: a potential link between signal transduction and RNA stability. *Mol. Cell. Biol.* **18**, 3956–3965.
- Ganesh, C., Shah, A. N., Swaminathan, C. P., Suroliya, A. and Varadarajan, R. (1997). Thermodynamic characterization of the reversible, two-state unfolding of maltose binding protein, a large two-domain protein. *Biochemistry* **36**, 5020–5028.
- Ghosh, H. S., Reizis, B. and Robbins, P. D. (2011). SIRT1 associates with eIF2- $\alpha$  and regulates the cellular stress response. *Sci. Rep.* **1**, 150.
- Haigis, M. C. and Guarente, L. P. (2006). Mammalian sirtuins—emerging roles in physiology, aging, and calorie restriction. *Genes Dev.* **20**, 2913–2921.
- Irvine, K., Stirling, R., Hume, D. and Kennedy, D. (2004). Rasputin, more promiscuous than ever: a review of G3BP. *Int. J. Dev. Biol.* **48**, 1065–1077.
- Jedrusic, M. A. and Schulze, E. (2003). Telomeric position effect variegation in *Saccharomyces cerevisiae* by *Caenorhabditis elegans* linker histones suggests a mechanistic connection between germ line and telomeric silencing. *Mol. Cell. Biol.* **23**, 3681–3691.
- Jedrusic, M. A. and Schulze, E. (2007). Linker histone HIS-24 (H1.1) cytoplasmic retention promotes germ line development and influences histone H3 methylation in *Caenorhabditis elegans*. *Mol. Cell. Biol.* **27**, 2229–2239.
- Jiang, H., Khan, S., Wang, Y., Charron, G., He, B., Sebastian, C., Du, J., Kim, R., Ge, E., Mostoslavsky, R. et al. (2013). SIRT6 regulates TNF- $\alpha$  secretion through hydrolysis of long-chain fatty acyl lysine. *Nature* **496**, 110–113.
- Jud, M. C., Czerwinski, M. J., Wood, M. P., Young, R. A., Gallo, C. M., Bickel, J. S., Petty, E. L., Mason, J. M., Little, B. A., Padilla, P. A. et al. (2008). Large P body-like RNPs form in *C. elegans* oocytes in response to arrested ovation, heat shock, osmotic stress, and anoxia and are regulated by the major sperm protein pathway. *Dev. Biol.* **318**, 38–51.
- Kaidi, A., Weinert, B. T., Choudhary, C. and Jackson, S. P. (2010). Human SIRT6 promotes DNA end resection through CtIP deacetylation. *Science* **329**, 1348–1353.
- Kanfi, Y., Naiman, S., Amir, G., Peshti, V., Zinman, G., Nahum, L., Bar-Joseph, Z. and Cohen, H. Y. (2012). The sirtuin SIRT6 regulates lifespan in male mice. *Nature* **483**, 218–221.
- Kawaguchi, Y., Kovacs, J. J., McLaurin, A., Vance, J. M., Ito, A. and Yao, T. P. (2003). The deacetylase HDAC6 regulates aggresome formation and cell viability in response to misfolded protein stress. *Cell* **115**, 727–738.
- Kawahara, T. L., Michishita, E., Adler, A. S., Damian, M., Berber, E., Lin, M., McCord, R. A., Ongaigui, K. C., Boxer, L. D., Chang, H. Y. et al. (2009). SIRT6 links histone H3 lysine 9 deacetylation to NF- $\kappa$ B-dependent gene expression and organismal life span. *Cell* **136**, 62–74.
- Kedersha, N., Cho, M. R., Li, W., Yacono, P. W., Chen, S., Gilks, N., Golan, D. E. and Anderson, P. (2000). Dynamic shuttling of TIA-1 accompanies the recruitment of mRNA to mammalian stress granules. *J. Cell Biol.* **151**, 1257–1268.
- Kourtis, N. and Tavernarakis, N. (2011). Cellular stress response pathways and ageing: intricate molecular relationships. *EMBO J.* **30**, 2520–2531.
- Kwon, S. H., Zhang, Y. and Matthias, P. (2007). The deacetylase HDAC6 is a novel critical component of stress granules involved in the stress response. *Genes Dev.* **21**, 3381–3394.
- Lavinder, J. J., Hari, S. B., Sullivan, B. J. and Magliery, T. J. (2009). High-throughput thermal scanning: a general, rapid dye-binding thermal shift screen for protein engineering. *J. Am. Chem. Soc.* **131**, 3794–3795.
- Lavut, A. and Raveh, D. (2012). Sequestration of highly expressed mRNAs in cytoplasmic granules, P-bodies, and stress granules enhances cell viability. *PLoS Genet.* **8**, e1002527.
- Mao, Z., Hine, C., Tian, X., Van Meter, M., Au, M., Vaidya, A., Seluanov, A. and Gorbunov, V. (2011). SIRT6 promotes DNA repair under stress by activating PARP1. *Science* **332**, 1443–1446.
- McCord, R. A., Michishita, E., Hong, T., Berber, E., Boxer, L. D., Kusumoto, R., Guan, S., Shi, X., Gozani, O., Burlingame, A. L. et al. (2009). SIRT6 stabilizes DNA-dependent protein kinase at chromatin for DNA double-strand break repair. *Aging* **1**, 109–121.
- Mello, C. C., Kramer, J. M., Stinchcomb, D. and Ambros, V. (1991). Efficient gene transfer in *C. elegans*: extrachromosomal maintenance and integration of transforming sequences. *EMBO J.* **10**, 3959–3970.
- Michishita, E., McCord, R. A., Berber, E., Kioi, M., Padilla-Nash, H., Damian, M., Cheung, P., Kusumoto, R., Kawahara, T. L., Barrett, J. C. et al. (2008). SIRT6 is a histone H3 lysine 9 deacetylase that modulates telomeric chromatin. *Nature* **452**, 492–496.
- Michishita, E., McCord, R. A., Boxer, L. D., Barber, M. F., Hong, T., Gozani, O. and Chua, K. F. (2009). Cell cycle-dependent deacetylation of telomeric histone H3 lysine K56 by human SIRT6. *Cell Cycle* **8**, 2664–2666.
- Mostoslavsky, R., Chua, K. F., Lombard, D. B., Pang, W. W., Fischer, M. R., Gellon, L., Liu, P., Mostoslavsky, G., Franco, S., Murphy, M. M. et al. (2006). Genomic instability and aging-like phenotype in the absence of mammalian SIRT6. *Cell* **124**, 315–329.
- Ohn, T. and Anderson, P. (2010). The role of posttranslational modifications in the assembly of stress granules. *WIREs RNA* **1**, 486–493.
- Parker, F., Maurier, F., Delumeau, I., Duchesne, M., Faucher, D., Debussche, L., Dugue, A., Schweighoffer, F. and Tocque, B. (1996). A Ras-GTPase-activating protein SH3-domain-binding protein. *Mol. Cell. Biol.* **16**, 2561–2569.
- Phillips, K. and de la Peña, A. H. (2011). The combined use of the ThermoFluor assay and ThermoQ analytical software for the determination of protein stability and buffer optimization as an aid in protein crystallization. *Curr. Protoc. Mol. Biol.* **10**, 1–15.
- Pitt, J. N., Schisa, J. A. and Priess, J. R. (2000). P granules in the germ cells of *Caenorhabditis elegans* adults are associated with clusters of nuclear pores and contain RNA. *Dev. Biol.* **219**, 315–333.
- Rappalber, J., Mann, M. and Ishihama, Y. (2007). Protocol for micro-purification, enrichment, pre-fractionation and storage of peptides for proteomics using StageTips. *Nat. Protoc.* **2**, 1896–1906.
- Rogina, B. and Helfand, S. L. (2004). Sir2 mediates longevity in the fly through a pathway related to calorie restriction. *Proc. Natl. Acad. Sci. USA* **101**, 15998–16003.
- Sanchez-Ruiz, J. M. (2010). Protein kinetic stability. *Biophys. Chem.* **148**, 1–15.
- Shevchenko, A., Tomas, H., Havlis, J., Olsen, J. V. and Mann, M. (2006). In-gel digestion for mass spectrometric characterization of proteins and proteomes. *Nat. Protoc.* **1**, 2856–2860.
- Sijen, T., Fleenor, J., Simmer, F., Thijsen, K. L., Parrish, S., Timmons, L., Plasterk, R. H. and Fire, A. (2001). On the role of RNA amplification in dsRNA-triggered gene silencing. *Cell* **107**, 465–476.
- Tennen, R. I., Berber, E. and Chua, K. F. (2010). Functional dissection of SIRT6: identification of domains that regulate histone deacetylase activity and chromatin localization. *Mech. Ageing Dev.* **131**, 185–192.
- Tissenbaum, H. A. and Guarente, L. (2001). Increased dosage of a sir-2 gene extends lifespan in *Caenorhabditis elegans*. *Nature* **410**, 227–230.
- Tourrière, H., Gallouzi, I. E., Chebli, K., Capony, J. P., Mouaikel, J., van der Geer, P. and Tazi, J. (2001). RasGAP-associated endoribonuclease G3BP: selective RNA degradation and phosphorylation-dependent localization. *Mol. Cell. Biol.* **21**, 7747–7760.
- Tourrière, H., Chebli, K., Zekri, L., Courselaud, B., Blanchard, J. M., Bertrand, E. and Tazi, J. (2003). The RasGAP-associated endoribonuclease G3BP assembles stress granules. *J. Cell Biol.* **160**, 823–831.
- Uniewicz, K. A., Ori, A., Xu, R., Ahmed, Y., Wilkinson, M. C., Fernig, D. G. and Yates, E. A. (2010). Differential scanning fluorimetry measurement of protein stability changes upon binding to glycosaminoglycans: a screening test for binding specificity. *Anal. Chem.* **82**, 3796–3802.
- Werner, E. D., Brodsky, J. L. and McCracken, A. A. (1996). Proteasome-dependent endoplasmic reticulum-associated protein degradation: an unconventional route to a familiar fate. *Proc. Natl. Acad. Sci. USA* **93**, 13797–13801.

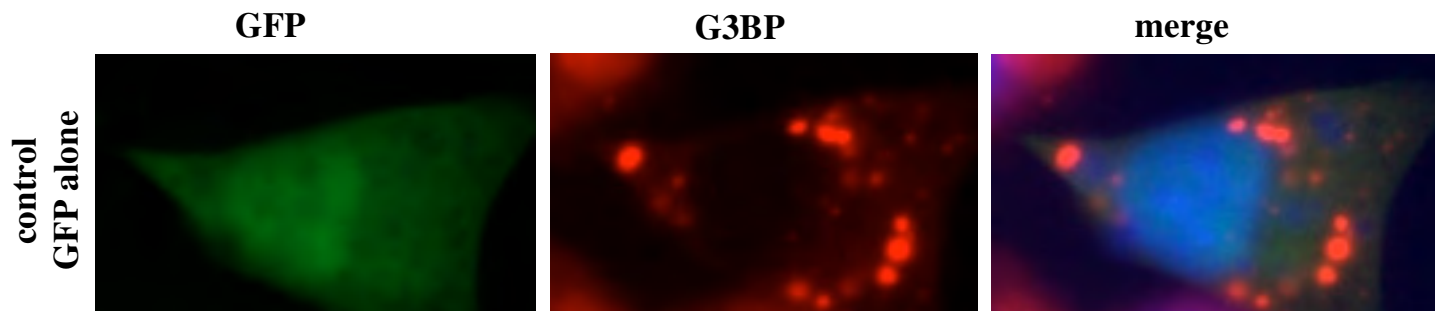


Fig. S1. GFP alone does not co-localize with G3BP in stressed NIH3T3 cells.

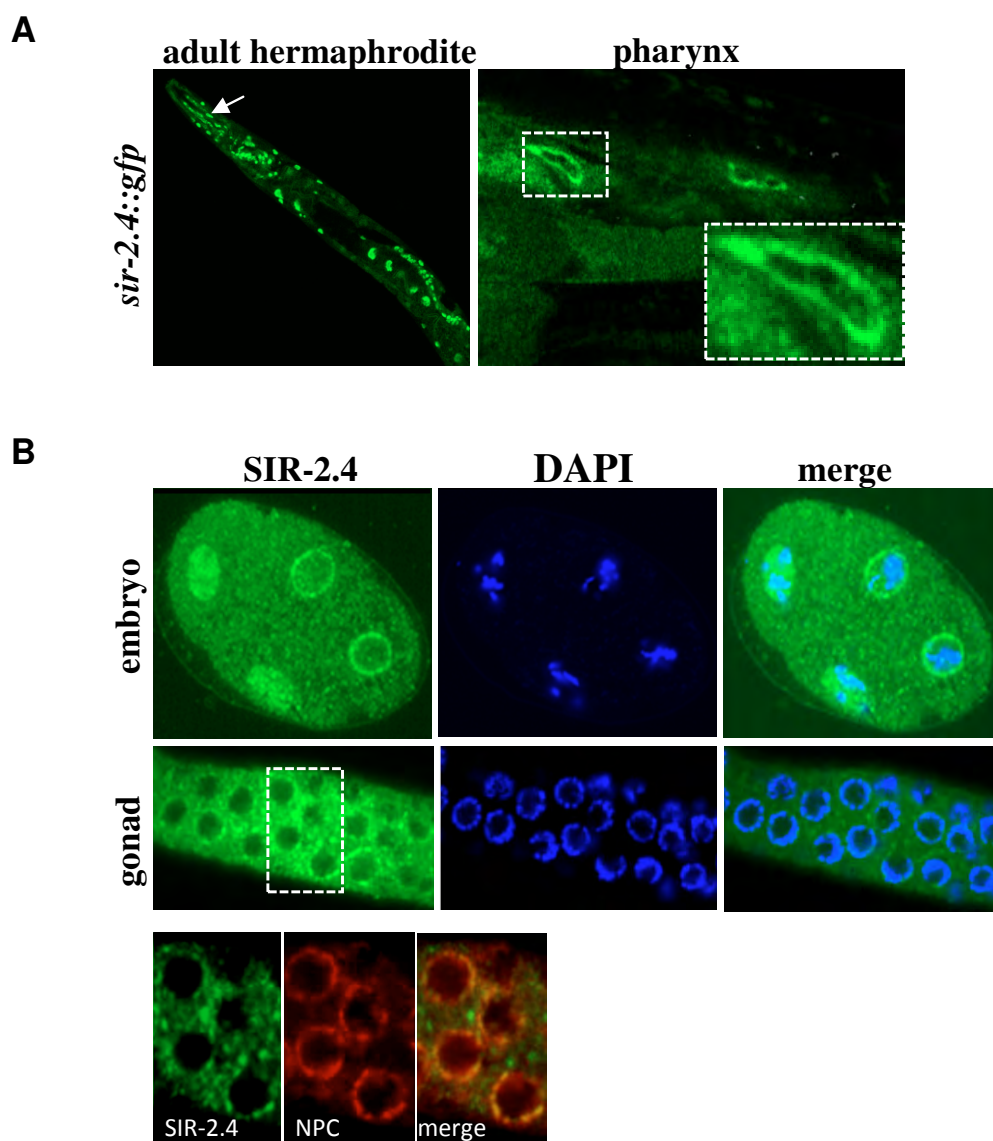
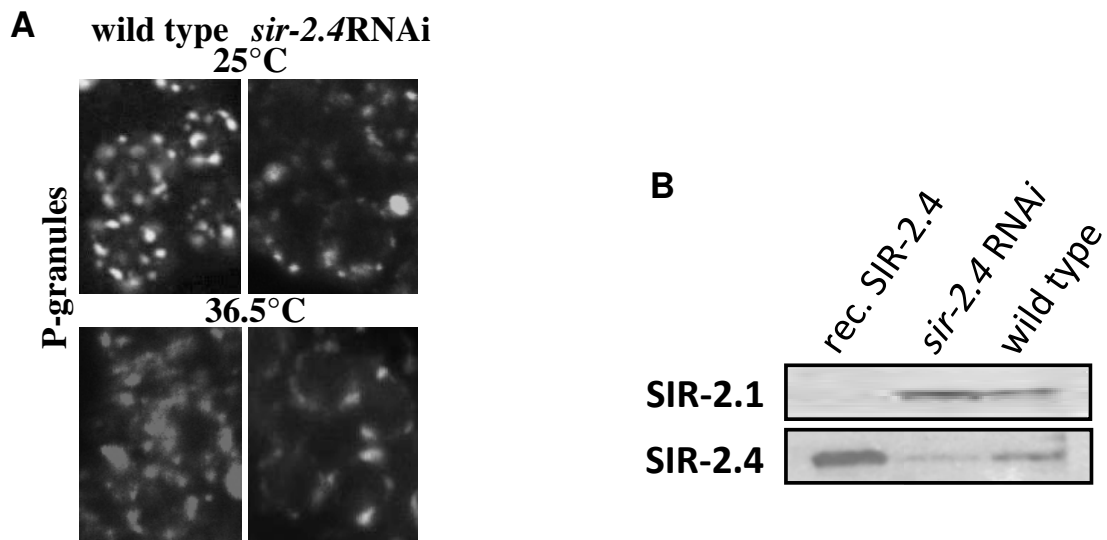
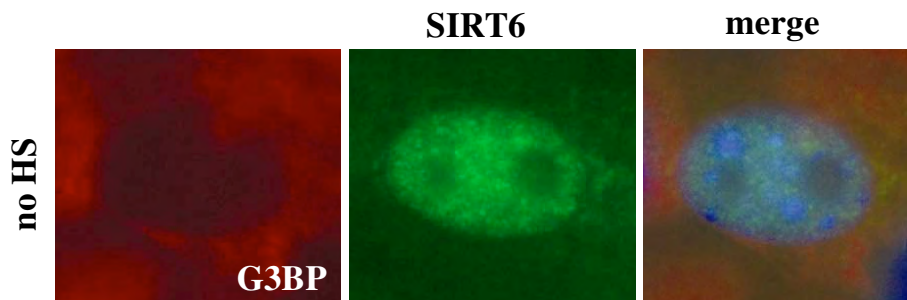


Fig. S2. SIR-2.4 is predominantly a nuclear envelope associated protein. (A, B) GFP-tagged SIR-2.4 protein (A) or endogenous SIR-2.4 is partially co-localized with nuclear pore complex (NPC) (B).



**Fig. S3.** SIR-2.4 influences number of P-granules. (A) Representative images of P-granules found in pachytene stage germline nuclei of wild type and *sir-2.4*-depleted 3-days old hermaphrodites at different temperatures. (B) Efficiency of *sir-2.4* knockdown. SIR-2.1 served as a loading control.



**Fig. S4.** Co-localization study of endogenous SIRT6 and G3BP in unstressed NIH3T3 cells.

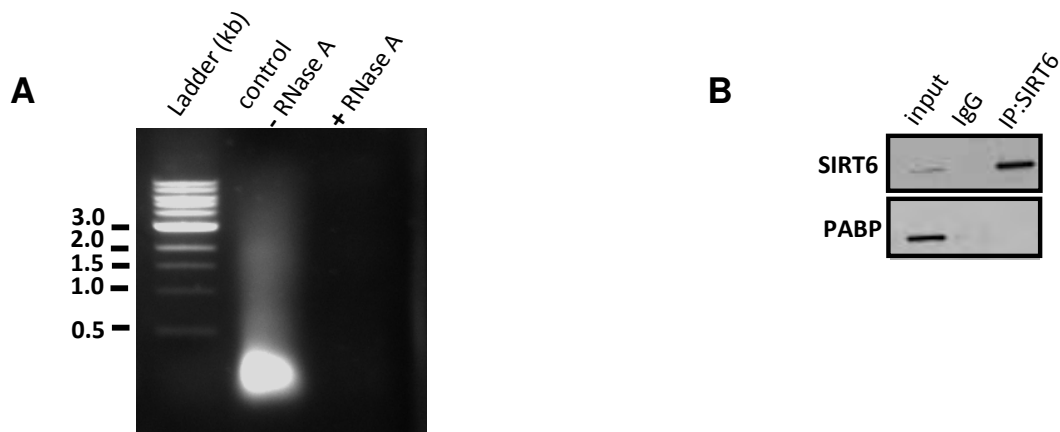


**Fig. S5.** (A) The effectiveness of RNase treatment in lysates prior to the immunoprecipitation assessed on agarose gel. (B) SIRT6 does not bind to *in vitro* translated PABP1.

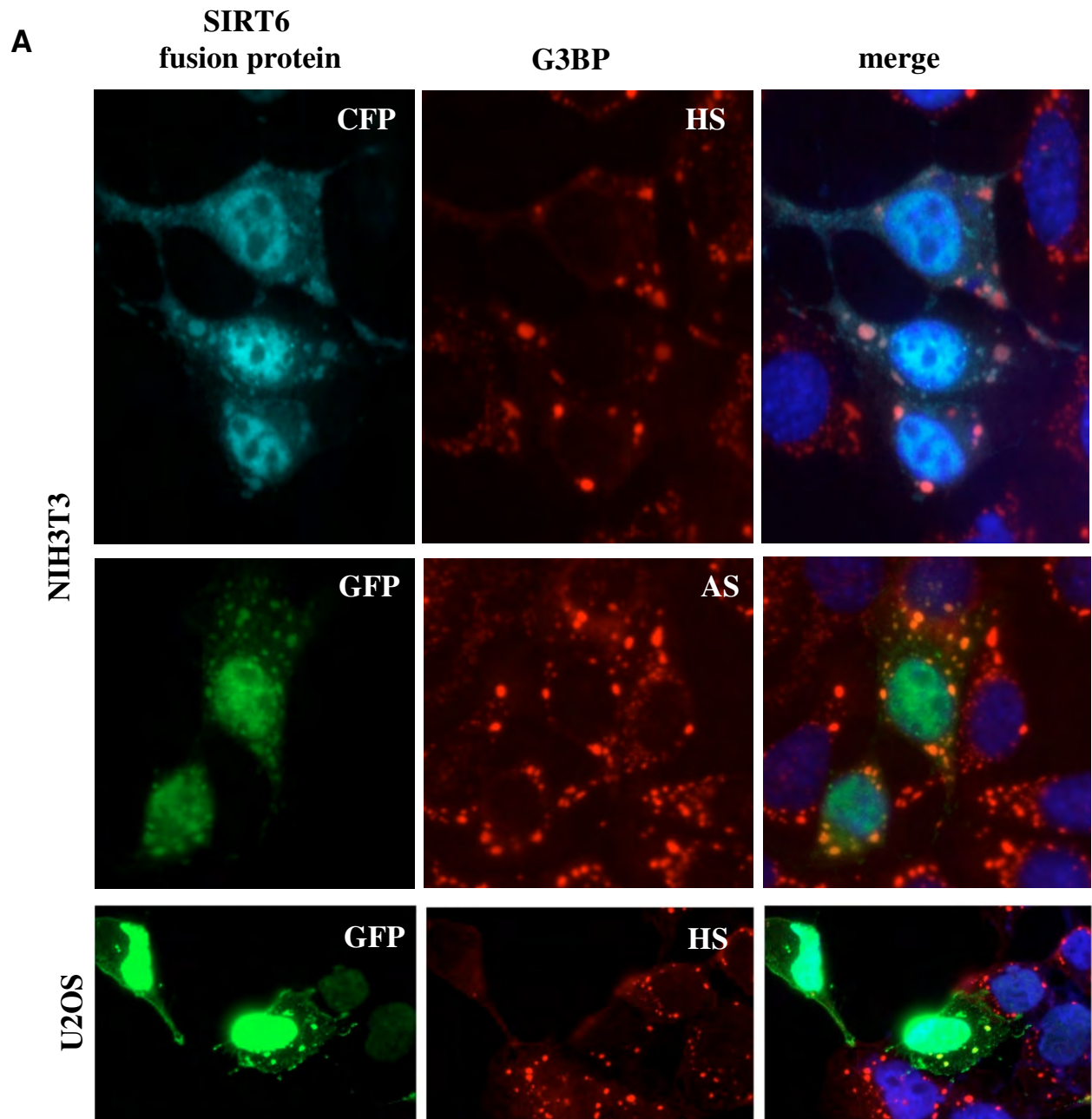


**Fig. S6.** SIRT6 localizes into SGs regardless of cell type or stress stimuli. (A) Co-localization study of CFP- or GFP-tagged SIRT6 protein with endogenous G3BP in stressed cells; HS for heat shock, AS for sodium arsenite.

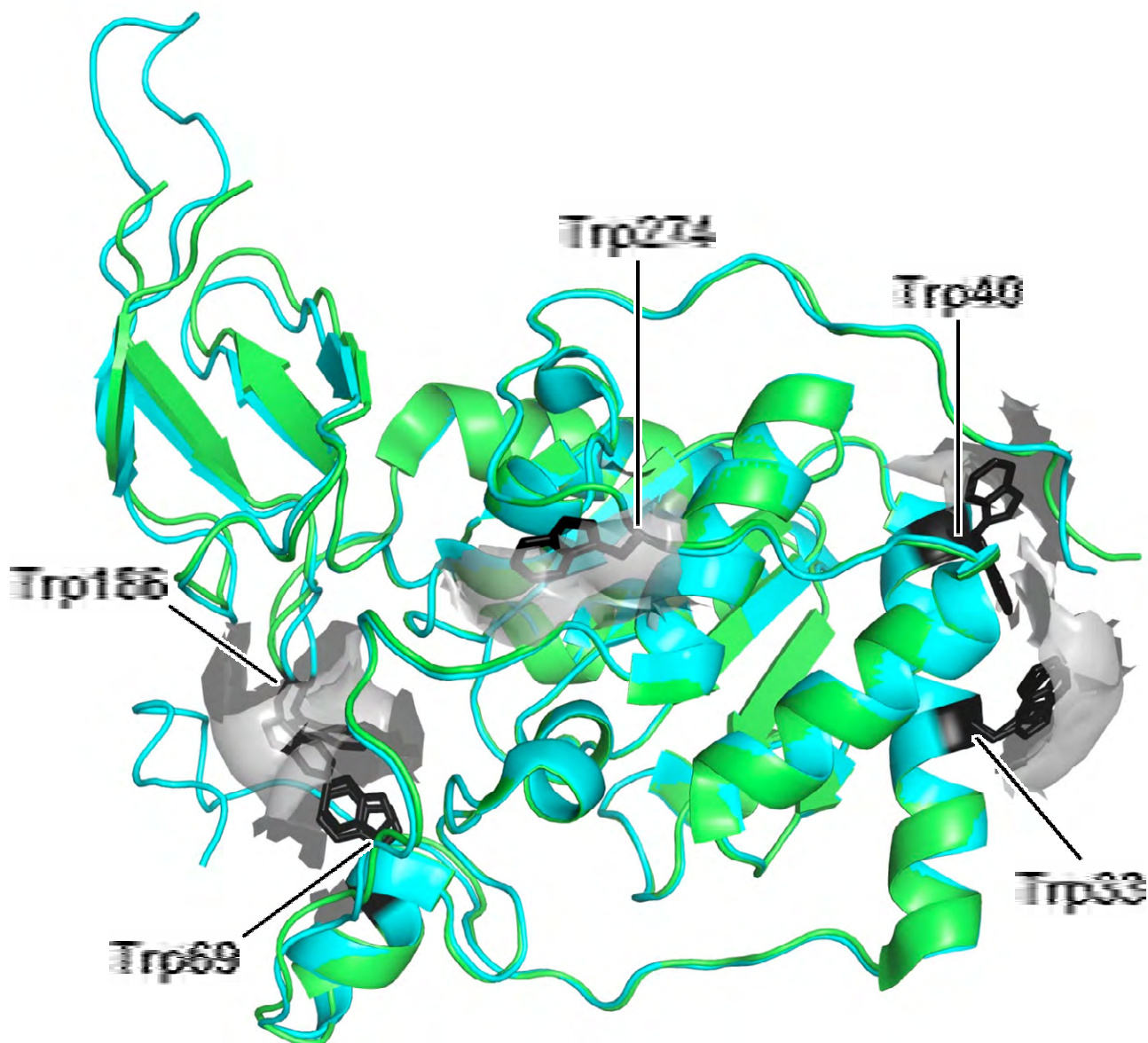


**Fig. S7.** Location of tryptophan residues in human SIRT6. Two crystal structures of human SIRT6 were globally aligned (PDB ID: 3K35, green & 3ZG6, cyan) with a root-mean-square deviation of 0.280 Å. Sidechains of tryptophan residues are shown in black with solvent-accessible surface in grey. Evidently, these residues except for Trp69 are located close to the protein surface. Molecular modeling and ray tracing were performed using Pymol (Schrödinger, LLC., USA).

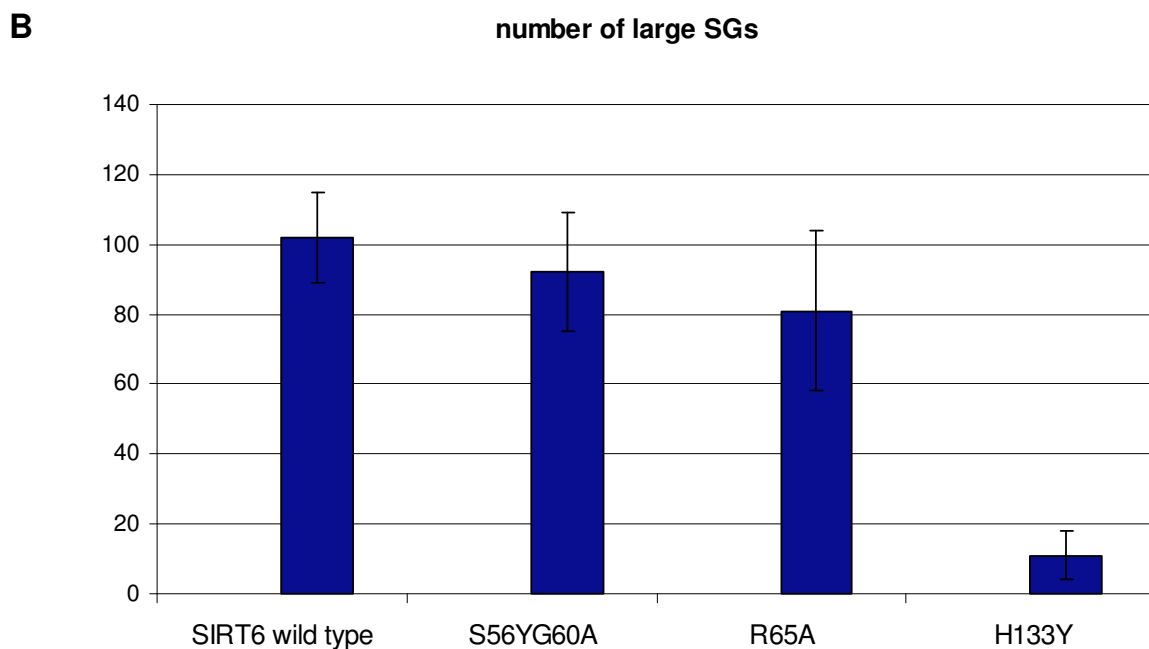
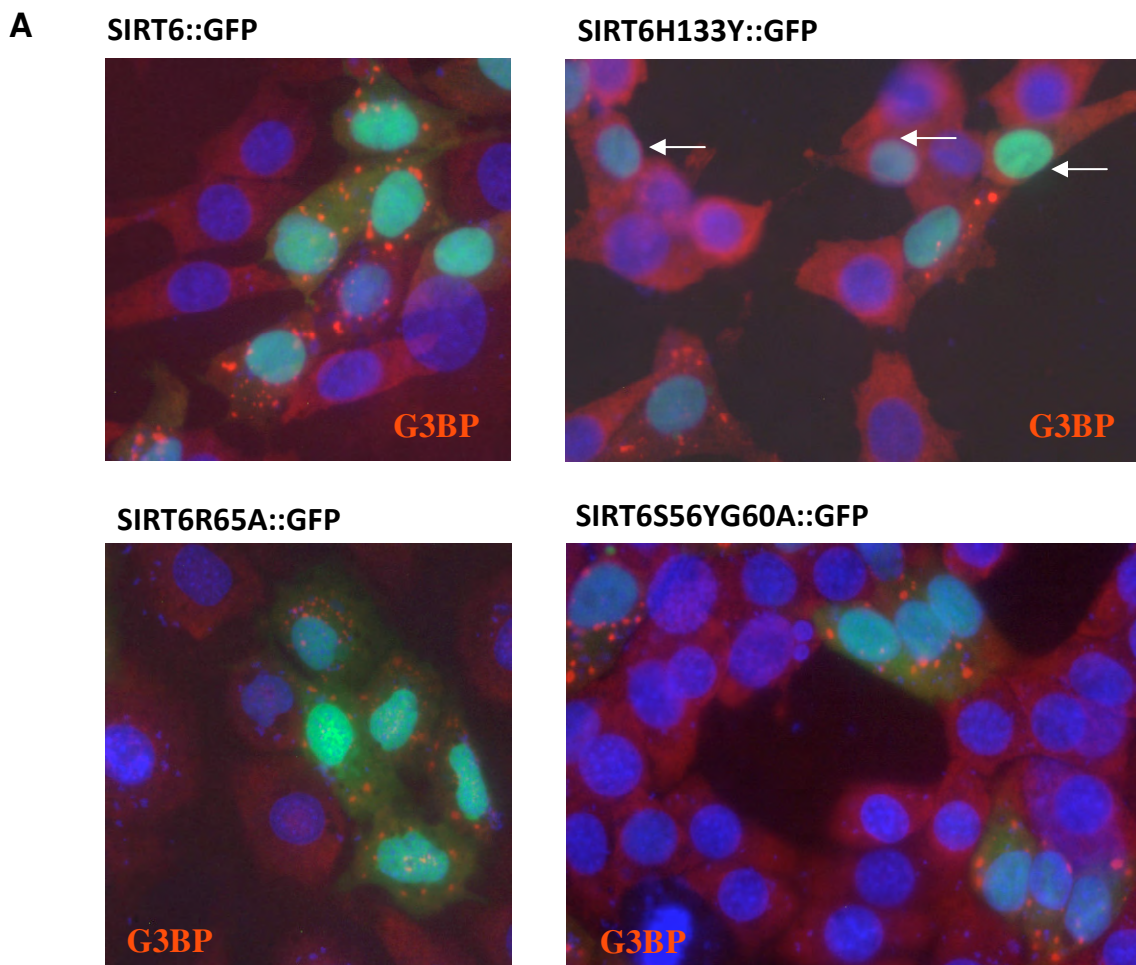


**Fig. S8. (A)** SIRT6 enzymatic activity induces G3BP formation. NIH3T3 cells, transfected with SIRT6::GFP and SIRT6::GFP constructs carrying point mutations, were fixed, stained with anti-G3BP antibody (red) without heat shock and analyzed for the presence of the G3BP stress granules. Arrows point at transfected cells with SIRT6H133Y plasmid (green fluorescence) without G3BP granules. **(B)** The graph shows the average size of G3BP granules. Analysis was based on 50 transfected cells. The large class of granules was identified on the basis of size (large - 31-230 pixels<sup>2</sup>). Results shown are mean values of three independent experiments, error bars, mean ± s.d.

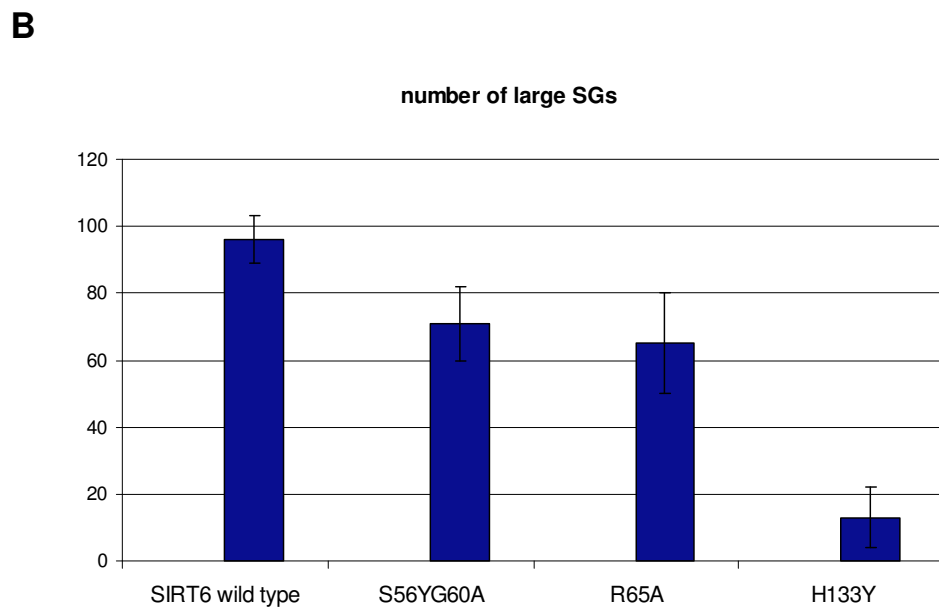
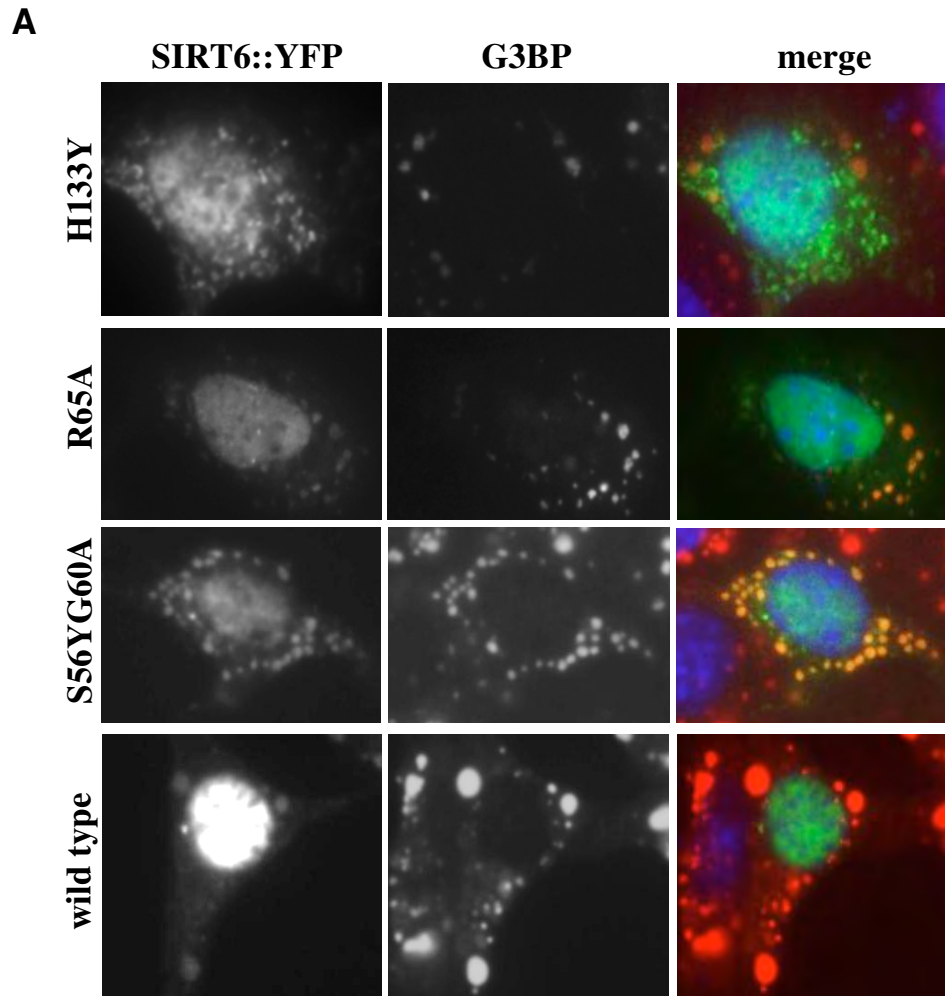
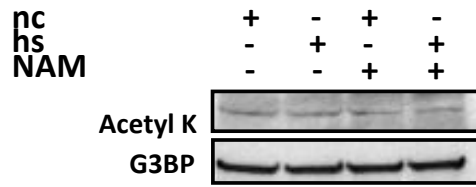
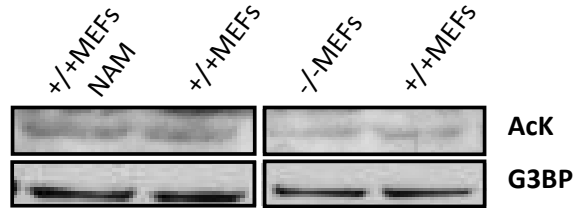


**Fig. S9.** (A) Deacetylase activity of SIRT6 influences the size of G3BP granules in stressed NIH3T3 cells. (A) Cells were transfected with SIRT6::GFP-point mutation constructs as indicated and analyzed 24 hours post-transfection for SGs formation using anti-G3BP antibody. (B) The graph shows the average size of SGs. Analysis was based on 50 transfected cells. The large class of granules was identified on the basis of size (large - 31-230 pixels<sup>2</sup>). Results shown are mean values of three independent experiments, error bars, mean ± s.d.

**A WB: NIH3T3 cell line**



**WB: MEFs cell line**



**B**

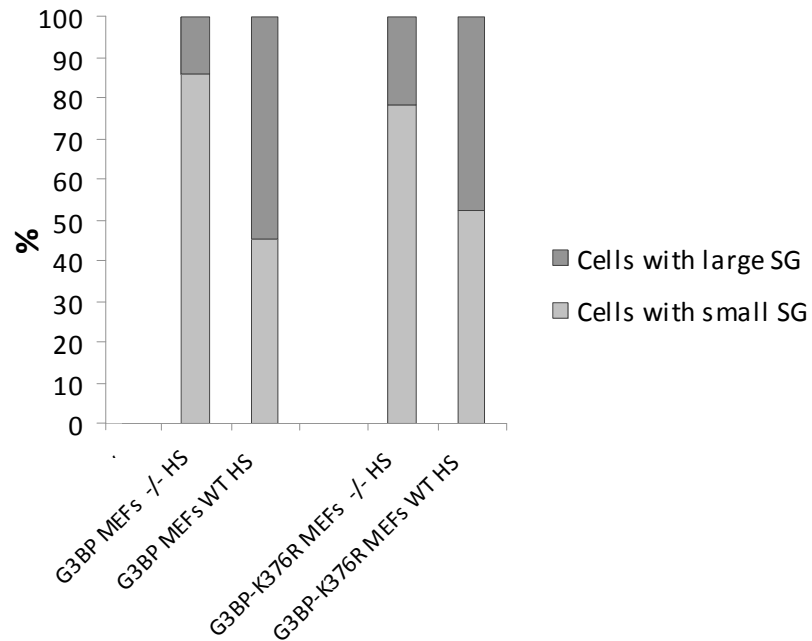


**Fig. S10.** SIRT6 does not influence the G3BP acetylation level. (A) Equal amounts of NIH3T3 or MEF cell lysates were analyzed on western blot. Deficiency of SIRT6 did not influence the acetylation level of G3BP. AcK for anti-acetylated lysine antibody; NAM for nicotinamide; nc for normal condition; hs for heat shock condition. (B) The graph represents the G3BP foci formation regarding the presence or absence of acetylation site at lysine 376.

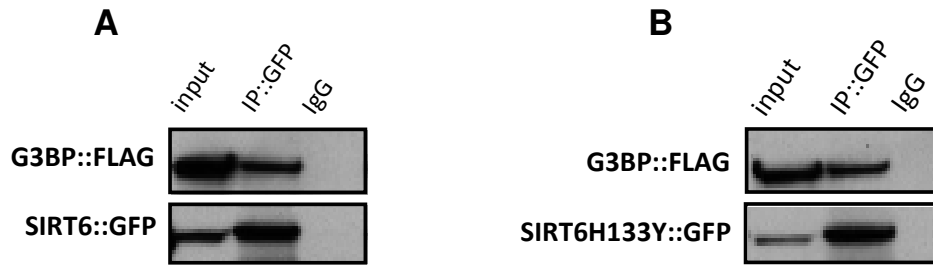


**Fig. S11.** SIRT6-G3BP association does not depend on SIRT6 enzymatic activity. (A, B) Western blot analysis showing co-immunoprecipitation of the SIRT6 wild type fusion protein (A) and catalytic-mutant SIRT6 (B) with G3BP.

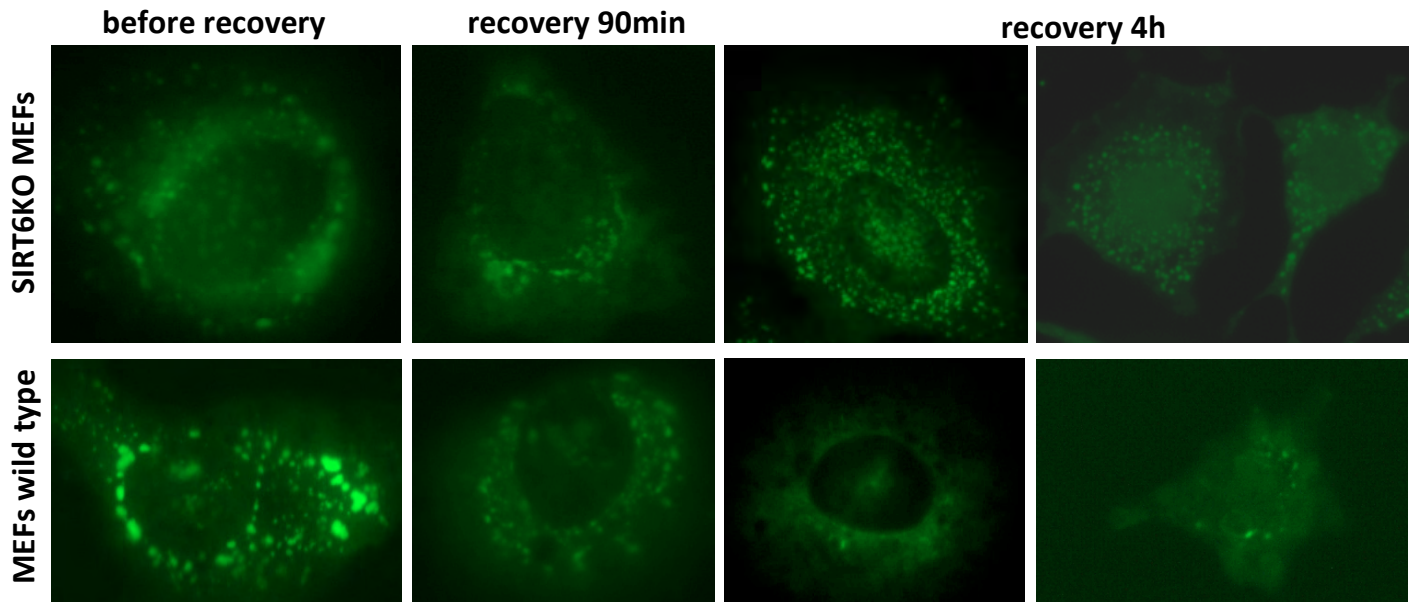


**Fig. S12.** SIRT6 impacts G3BP assembly. Representative images of stress granules in wild type (SIRT6<sup>+/+</sup>) and knockout (SIRT6<sup>-/-</sup>) MEFs cells. Both cell lines were transfected with G3BP::GFP, heat shock-treated and then incubated at 37°C. Finally, the cells were monitored for the size of stress granules before and after recovery by fluorescence microscopy.